Electronic Supplementary Information (ESI) for

Regioisomeric Effect on the Excited-State Fate Leading to Room-Temperature Phosphorescence or Thermally Activated Delayed Fluorescence in a Dibenzophenazine-Cored Donor–Acceptor–Donor System

Takumi Hosono,[a] Nicolas Oliveira Dcarli,[b] Paola Zimmermann Crocomo,[b] Tsuyoshi Goya,[c] Leonardo Evaristo de Sousa,[d] Norimitsu Tohnai,[a] Satoshi Minakata,[a] Piotr de Silva,[d] Przemyslaw Data,[b]* and Youhei Takeda[a]**

[a] Department of Applied Chemistry, Graduate School of Engineering, Osaka University, Yamadaoka 2-1, Suita, Osaka 565-0871, Japan
[b] Faculty of Chemistry, Silesian University of Technology, M. Strzody 9, 44-100 Gliwice, Poland
[c] New Business Commercialization Project, NIPPON SHOKUBAI CO., LTD., 5-8 Nishi Otabi-cho, Suita, Osaka 564-0034, Japan
[d] Department of Energy Conversion and Storage, Technical University of Denmark, Anker Engelunds Vej 301, 2800 Kongens Lyngby, Denmark

e-mail: pdes@dtu.dk; przemyslaw.data@polsl.pl; takeda@chem.eng.osaka-u.ac.jp

Table of Contents

General Remarks. All reactions were carried out under an atmosphere of nitrogen unless otherwise noted. Melting points were determined on a Stanford Research Systems MPA100 OptiMelt Automated Melting Point System. ^{1}H and ^{13}C spectra were recorded on a JEOL JMTC-400/54/SS Spectrometer (^{1}H NMR, 400 MHz; ^{13}C NMR, 100 MHz) using tetramethylsilane as an internal standard (δ = 0 ppm). ^{29}Si spectra were recorded on a Bruker AVANCE III 600 Spectrometer (119 MHz) using tetramethylsilane as an external standard (δ = 0 ppm). Infrared spectra were acquired on a SHIMADZU IRAffinity-1 FT-IR Spectrometer. Mass spectra and High-resolution mass spectra were obtained on a JEOL JMS-700 Mass Spectrometer. Cyclic voltammetry (CV) was performed with Biologic SP150 system. Thermogravimetric analysis (TGA) was performed with TG/DTA-7200 system (SII Nano Technology Inc.). Products were purified by chromatography on silica gel BW-300 and Chromatorex NH (Fuji Silysia Chemical Ltd.). Analytical thin-layer chromatography (TLC) was performed on pre-coated silica gel glass plates (Merck silica gel 60 F254 and Fuji Silysia Chromatorex NH, 0.25 mm thickness). Compounds were visualized with UV lamp.

Materials. 3,11-dibromodibenzo[*a,j*]phenazine (**8**) [CAS No. 1620543-64-7] was prepared according to the reported procedure.[S1] 7,7'-dibromo-1,1'-binaphthalene-2,2'-diamine (**11**, CAS No. 756822-96-5) was prepared according to the reported procedure.[S2] 2-Bromo-*N*-(2-bromophenyl)-*N*-(4-methoxybenzyl)aniline [CAS No. 1525711-66-3] and 10,10-diphenyl-5,10-dihydrodibenzo[*b*,*e*][1,4]azasiline [CAS No. 3508-62-1] were prepared according to the procedures in literature.[S3] 2,2'-Oxybis(bromobenzene) was prepared according to the procedure in literature.[S4] Commercial reagents were purchased (Sigma-Aldrich, TCI, or FUJIFILM Wako Pure Chemical Corp.) and used as received.

Photophysics. UV-vis spectra were recorded on a Shimadzu UV-2550 spectrophotometer. Steady-state emission spectra were recorded on a HAMAMATSU C11347-01 spectrometer with an integrating sphere and Jobin Yvon Horiba Fluorolog 3, with solvent studies performed in clean 1 cm path-length photoluminescence cuvettes (Arieka Cells) and temperature dependent film photoluminescence films studies performed on within a liquid N_2 cooled cryostat (Janis Research). Photoluminescence spectra were calibrated for detector efficiency using company supplied, instrument specific calibration files. The emitter materials was also degassed in toluene solvent using a custom made 1 cm path-length degassed cell stoppered with a Young tap and degassed using 5 freeze/thaw/pump cycles. The photoluminescence quantum yield (PLQY) of emitters in toluene solvent was determined using the reference method against 9,10-diphenylanthracene (DPA). Solid-state samples were prepared as 1% w/w ratio emitters in Zeonex® polymer host on clean/dry sapphire disc substrates. Phosphorescence, prompt fluorescence (PF), and delayed fluorescence (DF) spectra and decays were recorded using nanosecond gated luminescence and lifetime measurements (from 400 ps to 1 s) using either third harmonics of a high energy pulsed DPSS laser emitting at 355 nm (Q-Spark A50-TH-RE). Emission was focused onto a spectrograph and detected on a sensitive gated iCCD camera (Stanford Computer

Optics) having a sub-nanosecond resolution. PF/DF time-resolved measurements were performed by exponentially increasing gate and integration times. Temperature-dependent experiments were conducted using an helium cryostat (Janis Research) under a vacuum.

Devices. NPB (*N*,*N*′-di(1-naphthyl)-*N*,*N*′-diphenyl-(1,1′-biphenyl)-4,4′-diamine) was used as a Hole Injection Layer (HIL) and Hole Transport Layer (HTL), TSBPA (4,4'-(Diphenylsilanediyl)bis(N,N-diphenylaniline)) and TAPC (4,4′-Cyclohexylidenebis[*N*,*N*-bis(4-methylphenyl)benzenamine]) were used as a Electron Blocking Layer (EBL). TPBi 2,2',2"-(1,3,5-Benzinetriyl)-tris(1-phenyl-1-H-benzimidazole) was introduced as an Electron Transport Layer (ETL). Lithium fluoride (LiF) and aluminium were used as the cathode. Organic semiconductors and aluminium were deposited at a rate of 1 Ås-1, and the LiF layer was deposited at 0.1 Ås-1. TCTA (Tris(4-carbazoyl-9-ylphenyl)amine) and CBP 4,4′-bis(*N*-carbazolyl)-1,1′-biphenyl, were used as hosts for all emitters. All materials were purchased from Sigma Aldrich or Lumtec and were purified by temperature-gradient sublimation in a vacuum. OLEDs have been fabricated on pre-cleaned, patterned indium-tin-oxide (ITO) coated glass substrates with a sheet resistance of 20 Ω/sq and ITO thickness of 100 nm. All small molecules and cathode layers were thermally evaporated in a Kurt J. Lesker SuperSpectros 200 evaporation system under pressure of 10^{-7} mbar without breaking the vacuum. The sizes of pixels were 4 mm^2, 8 mm^2 and 16 mm^2. Each emitting layer has been formed by co-deposition of dopant and host at the specific rate to obtain 10% content of the emitter. The characteristics of the devices were recorded using a 6-inch integrating sphere (Labsphere) inside the glovebox connected to a Source Meter Unit and Ocean Optics USB4000 spectrometer.

Electrochemistry. Electrochemical measurements were performed in 0.1 M Bu_4NPF_6 (99%, Sigma Aldrich, dried) in dichloromethane (CHROMASOLV®, 99.9% Sigma Aldrich). Solutions were purged with argon prior to measurement. Electrodes: working (Pt disc 1 mm of diameter), counter (Pt wire), reference (Ag/AgCl calibrated against ferrocene).

Synthetic Procedures and Spectroscopic Data of New Compounds.

Synthesis tic procedures for 2,12-dibromo-dibenzo[a,j]phenazine (**12**)

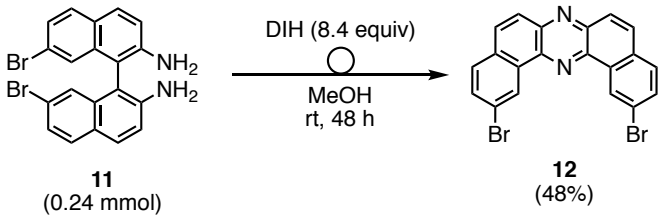

11
(0.24 mmol)

12
(48%)

To a two-necked round-bottomed flask (50 mL) equipped with a magnetic stir bar, was added 7,7'-dibromo-1,1'-binaphthalene-2,2'-diamine (**11**) (106.3 mg, 0.24 mmol) under the air. The vessel was capped with a rubber septum and evacuated and refilled with N_2 gas for three times. Methanol (20 mL) was added under a stream of N_2 gas, and the solution was stirred for 2 h at room temperature to

solve the diamine. To the mixture, was added 1,3-diiodo-5,5-dimethylhydantoin (764.3 mg, 2.01 mmol, 8.4 equiv) under a stream of N_2 gas for 48 h before quenched with aqueous $Na_2S_2O_3$ (1.0 M, 20 mL), and the resulting mixture was extracted with $CHCl_3$ (20 mL × 3). The combined organic extracts were dried over Na_2SO_4, and the solvent was evaporated in vacuo to give the crude product, which was purified by flash column chromatography on silica gel (eluent: *n*-hexane/$CHCl_3$ 8:2) followed by recrystallization from $CHCl_3$, affording the title compound **12** as yellow solid (50.4 mg, 0.12 mmol, 48%). Mp 313 °C (dec.); R_f 0.31 (*n*-hexane/EtOAc 8:2, NH silica); ^{1}H NMR (400 MHz, $CDCl_3$): δ 9.72 (d, J = 1.6 Hz, 2H), 8.06–8.12 (m, 4H), 7.93 (dd, J = 8.6, 1.8 Hz, 2H), 7.87 (d, J = 8.4 Hz, 2H); ^{13}C NMR (100 MHz, $CDCl_3$): δ 143.2, 139.5, 137.7, 132.7, 132.5, 132.1, 129.7, 127.9, 127.4, 122.5; IR (ATR): ν 3059, 3037, 1591, 1506, 1425, 1344, 1323, 1030, 897, 825, 793, 754 cm^{-1}; MS (EI): *m/z* (relative intensity, %) 440 ([M+4]$^+$, 50), 438 ([M+2]$^+$, 100), 436 (M$^+$, 50), 359 ([M+2–Br]$^+$, 11), 357 ([M–Br]$^+$, 11), 278 ([M–2Br]$^+$, 22), 139 ([$C_{10}H_5N$]$^+$, 19); HRMS (EI): *m/z* calcd for $C_{20}H_{10}Br_2N_2$ (M$^+$) 435.9211, found 435.9216.

Synthetic procedures for 10,10-diisopropyl-5,10-dihydrodibenzo[b,e][1,4]azasiline (**9**) [CAS No. 2240184-18-1]

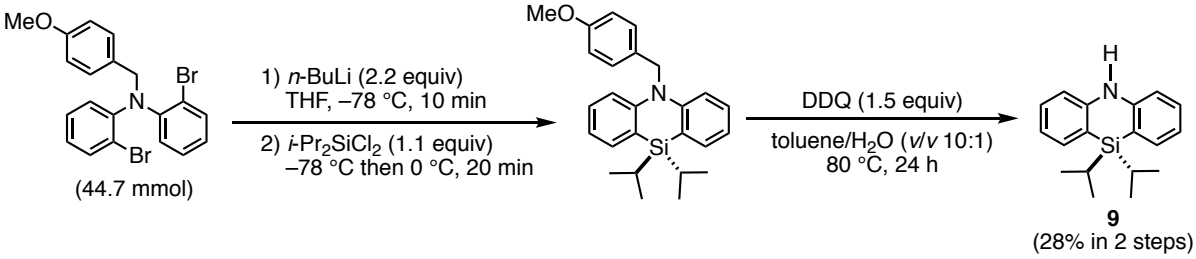

The 500 mL three-necked round-bottomed flask equipped with a magnetic stirring bar, a three-way cock, and two septum was flame-dried under vacuum and refilled with an Ar atmosphere. To the flask, were added 2-bromo-*N*-(2-bromophenyl)-*N*-(4-methoxybenzyl)aniline (20 g, 44.7 mmol, 1.0 equiv) and THF (200 mL). The resulting solution was stirred at room temperature for 5 min. The flask was cooled to –78 °C, and *n*-BuLi [63 mL, 98.3 mmol, 1.55 M (*n*-hexane solution), 2.2 equiv] was added dropwise to the solution over 10 min. The reaction mixture was stirred at –78 °C for 10 min, and dichlorodiisopropylsilane (8.8 mL, 9.10 g, 49.1 mmol, 1.1 equiv) dissolved in THF (40 mL) was added to it dropwise over 10 min. After the mixture was stirred at –78 °C for 20 min, the flask was submerged into an ice bath. The mixture was stirred at 0 °C for 20 min, and aq. $NaHCO_3$ (5%, 200 mL) was added to it over 10 min. Organic layer was separated, washed with brine (200 mL), and dried over Na_2SO_4, which was then dried by evaporating organic solvents under reduced pressure to give crude product as brown oil (23.5 g). The crude product was purified by flash column chromatography on an NH silica gel (eluent: heptane) to provide 10,10-diisopropyl-5-(4-methoxybenzyl)-5,10-dihydrodibenzo[*b*,*e*][1,4]azasiline as white solid (16.0 g). R_f 0.28 (*n*–heptane/toluene 10:1, silica). This intermediate was subsequently subjected to the next reaction without further purification.

To a 500 mL flask, were added 10,10-diisopropyl-5-(4-methoxybenzyl)-5,10-dihydrodibenzo[*b*,*e*][1,4]azasiline (15.9 g, 39.5 mmol, 1.0 equiv), DDQ (9.88 g, 43.5 mmol, 1.1 equiv), toluene, (159 mL), and distilled water (15.9 mL). The flask was stirred at 80 °C for 22 h. Another portion of DDQ (3.59 g, 15.8 mmol, 0.4 equiv) was added to the reaction mixture, and the resulting mixture was stirred for 2 h. The reaction mixture was allowed to cool to room temperature, and aq. $NaHCO_3$ (5%, 159 mL) was added dropwise to it over 30 min. The resulting mixture was stirred at room temperature for 15 min, and the precipitates were filtered and washed with toluene (90 mL). The filtrate was separated into organic and aqueous layers with a separatory funnel. The organic layer was washed with brine (80 mL), dried over Na_2SO_4. Organic solvents were evaporated under reduced pressure to give crude product as dark brown oil (16.2 g). The crude product was purified by flash column chromatography on an NH silica gel (eluent: heptane/toluene = 10:1 to 5:1) to give orange oil (6.63 g) and orange solid (3.12 g). The obtained oil and solid were combined and once again purified by flash chromatography on an NH silica gel (eluent: heptane) to give orange solid (5.47 g). The solid was further purified by recrystallization from pentane solution to give the title compound as yellow solid (3.54 g, 12.5 mmol, 28% in 2 steps). Mp 141 °C (dec.); R_f 0.60 (*n*-hexane/EtOAc 8:2, NH silica); ^{1}H NMR (400 MHz, $CDCl_3$): δ 7.48 (dd, J = 7.6, 1.2 Hz, 2H), 7.28 (dd, J = 7.6, 7.6 Hz, 2H), 6.89 (dd, J = 7.4, 7.4 Hz, 2H), 6.73 (d, J = 8.0 Hz, 2H), 6.41 (brs, 1H), 1.37 (sep, J = 7.2 Hz, 2H), 1.01 (d, J = 7.2 Hz, 12H); ^{13}C NMR (100 MHz, $CDCl_3$): δ 135.0, 130.1, 119.1, 114.9, 113.4, 103.9, 18.1, 13.0; ^{29}Si NMR (119 MHz, $CDCl_3$): δ –16.2; IR (ATR): ν 3398, 2939, 2862, 1600, 1568, 1449, 1435, 1335, 1238, 1220, 991, 883, 750 cm^{-1}; MS (EI): *m/z* (relative intensity, %) 282 ([M+1]$^+$, 7), 281 (M$^+$, 31), 238 ([M–^{i}Pr]$^+$, 100), 210 ([$C_{13}H_{12}Nsi$]$^+$, 30), 195 ([M–2^{i}Pr]$^+$, 6), 180 ([$C_{12}H_8Si$]$^+$, 16); HRMS (EI): *m/z* calcd for $C_{18}H_{23}Nsi$ (M$^+$) 281.1600, found 281.1605. Anal. Calcd for $C_{18}H_{23}Nsi$: C, 76.81; H, 8.24; N, 4.98. Found: C, 76.90; H, 8.43; N, 5.00.

Synthetic procedures for 5H-spiro[dibenzo[b,e][1,4]azasiline-10,10'-dibenzo[b,e][1,4]oxasiline] (**10**)

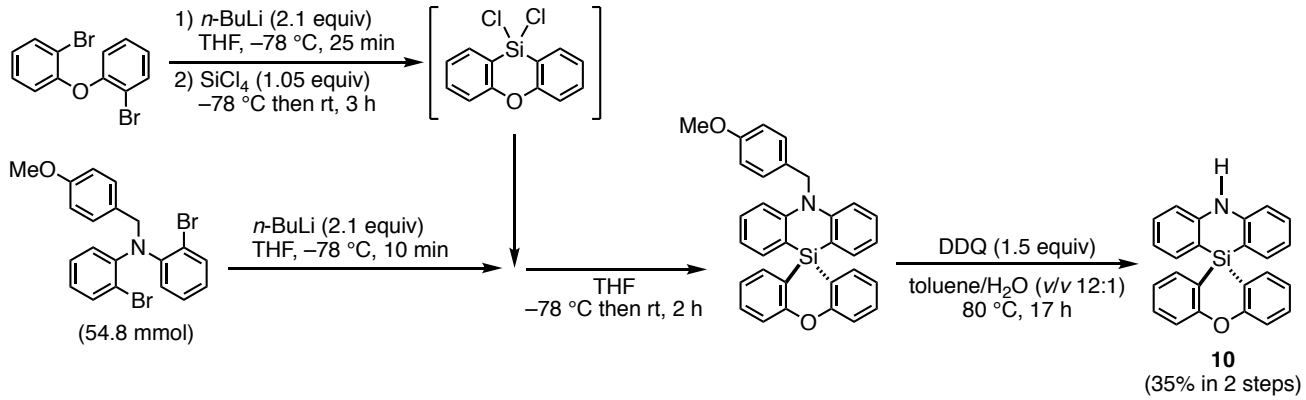

The 500 mL three-necked round-bottomed flask equipped with a magnetic stirring bar, a three-way cock, and two septum was flame-dried under vacuum and refilled with an Ar atmosphere. To the flask, were added 2,2'-oxybis(bromobenzene) (20 g, 60.9 mmol, 1.0 equiv) and THF (200 mL).

The resulting solution was stirred at room temperature for 15 min. The reaction mixture was cooled to –78 °C, and *n*-BuLi [82 mL, 128 mmol, 1.55 M (*n*-hexane solution), 2.1 equiv] was added to it dropwise over 10 min. The resulting mixture was stirred for 25 min. To the solution, $SiCl_4$ (7.3 mL, 10.8 g, 64.0 mmol, 1.05 equiv) in THF (40 mL) was added dropwise to it over 10 min to generate white suspension, which was then stirred for 10 min. The reaction mixture was allowed to warm up to room temperature and stirred for 3 h. The suspension was filtered, and the filtrate was concentrated under reduced pressure to give pale brown solid (21.0 g). The solid was dissolved in $CHCl_3$ (200 mL), the precipitates were filtered, and the filtrate was concentrated under reduced pressure to afford 10,10-dichloro-10*H*-dibenzo[*b*,*e*][1,4]oxasiline as pale yellow solid (17.4 g). This intermediate was subsequently subjected to the next reaction without further purification.

The 1 L three-necked round-bottomed flask equipped with a magnetic stirring bar, a three-way cock, and two septum was flame-dried under vacuum and refilled with an Ar atmosphere. To the flask, were added 2-bromo-*N*-(2-bromophenyl)-*N*-(4-methoxybenzyl)aniline (24.5 g, 54.8 mmol, 1.0 equiv) and THF (245 mL), and the resulting solution was stirred at room temperature for 15 min. The flask was cooled to –78 °C, and *n*-BuLi [74 mL, 115 mmol, 1.55 M (*n*-hexane solution), 2.1 equiv] was added dropwise to it over 10 min, and the resulting mixture was stirred for 10 min. To the mixture, 10,10-dichloro-10*H*-dibenzo[*b*,*e*][1,4]oxasiline (16.0 g) in THF (50 mL) was added dropwise over 10 min to give pale brown solution. The solution was stirred for 5 min and allowed to warm to room temperature and stirred for 2 h. To a cold aq. $NaHCO_3$ (300 mL) at 0 °C, the reaction mixture was added dropwise through a cannula. The resulting mixture was stirred at 0°C for 20 min. Organic layer was separated and washed with brine (250 mL) to give precipitates. The precipitates were filtered and dissolved in $CHCl_3$ (300 mL), which was combined with the organic layer. To the aqueous layer, distilled water (200 mL) was added to solve precipitates, and the aqueous layer was extracted with toluene (200 mL) to combine with the organic layer. The combined organic layer was dried over Na_2SO_4, and organic solvents were evaporated under reduced pressure to afford reddish-brown slurry (50.0 g). The slurry was purified by flash column chromatography on an NH silica gel (eluent: heptane/toluene = 20:1 to 10:1 to 3:1) to afford while solid (23.4 g). R_f 0.33 (*n*–heptane/toluene 2:1, silica). This intermediate was subsequently subjected to the next reaction without further purification.

To a 1 L flask, were added 5-(4-methoxybenzyl)-5*H*-spiro[dibenzo[*b*,*e*][1,4]azasiline-10,10'-dibenzo[*b*,*e*][1,4]oxasiline] (25.0 g, 51.6 mmol, 1.0 equiv) and toluene (300 mL). The resulting mixture was heated at 80 °C to solve the solid. To the solution, distilled water (25 mL) and DDQ (17.6 g, 77.5 mmol, 1.5 equiv) were added, and the resulting mixture was stirred at 80 °C for 17 h. The reaction mixture was allowed to cool to room temperature and poured into aq. $NaHCO_3$ (5%, 500 mL), and the resulting mixture was stirred for 35 min and filtered. From the filtrate, organic layer was separated and washed with brine (300 mL) and dried over Na_2SO_4. Organic solvents were evaporated under reduced pressure to give brown solid (24.2 g), which was purified by flash column

chromatography on an NH silica gel (eluent: heptane/toluene = 5:1) to give yellow solid (9.04 g). To the obtained yellow solid, heptane (80 mL) was added, and the suspension was stirred under reflux condition, allowed to cool to room temperature, and filtered to give pale yellow solid (7.30 g). To the solid, MeOH (75 mL) was added, and the suspension was stirred at room temperature for 20 min and filtered to give pale greenish yellow solid (7.15 g). To the solid, EtOH (70 mL) was added, and the suspension was stirred under reflux condition, allowed to cool to room temperature, and filtered to give the title compound (**10**) as pale greenish yellow solid (6.91 g, 19.0 mmol, 35% in 2 steps). Mp 307 °C (dec.); R_f 0.22 (*n*-hexane/EtOAc 8:2, NH silica); ^{1}H NMR (400 MHz, CD_2Cl_2) δ 7.45 (ddd, J = 8.0, 7.6, 2.0 Hz, 2H), 7.36 (ddd, J = 6.8, 6.8, 1.4 Hz, 2H), 7.29 (d, J = 8.4 Hz, 2H), 7.26 (dd, J = 7.4, 1.8 Hz, 2H), 7.21 (dd, J = 7.4, 1.4 Hz, 2H), 7.04 (ddd, J = 7.2, 6.8, 0.8 Hz, 2H), 6.95–6.98 (m, 3H), 6.83 (dd, J = 7.6, 7.2 Hz, 2H); ^{13}C NMR (100 MHz, $CDCl_3$): δ 160.5, 146.9, 136.75, 136.70, 136.3, 131.6, 131.19, 122.7, 120.0, 117.7, 115.18, 115.17; ^{29}Si NMR (119 MHz, $CDCl_3$): δ –49.2; IR (ATR): ν 3377, 3051, 3009, 1570, 1456, 1419, 1340, 1263, 1207, 1130, 1074, 881, 746 cm^{-1}; MS (EI): *m/z* (relative intensity, %) 364 ([M+1]$^+$, 32), 363 (M$^+$, 100), 286 ([M–Ph]$^+$, 2), 195 ([M–$C_{12}H_8O$]$^+$, 13), 167 ([$C_{12}H_9N$]$^+$, 23); HRMS (EI): *m/z* calcd for $C_{24}H_{17}NOSi$ (M$^+$) 363.1079, found 363.1079. Anal. Calcd for $C_{24}H_{17}NOSi$: C, 79.30; H, 4.71; N, 3.85. Found: C, 79.00; H, 4.71; N, 3.75.

Synthetic procedures for 3,11-bis(10,10-diisopropyldibenzo[b,e][1,4]azasilin-5(10H)-yl)dibenzo[a,j]phenazine (**2**)

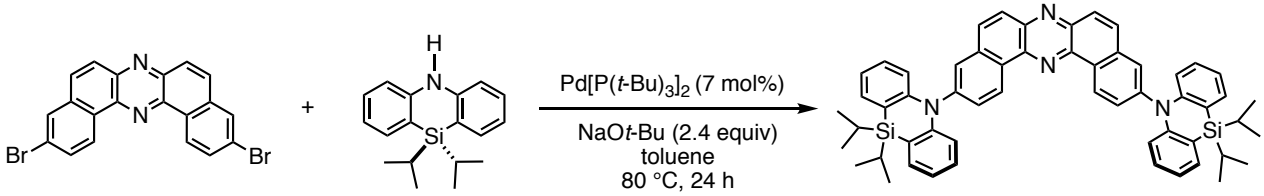

8 (0.10 mmol) + **9** (2.2 equiv) → **2** (55%)

A two-necked reaction tube (10 mL) equipped with a magnetic stir bar was transferred into a glove box. To the tube, were added Pd[P(*t*-Bu)$_3$]$_2$ (3.1 mg, 6.0 μmol, 7 mol%) and NaO*t*-Bu (21 mg, 0.22 mmol, 2.4 equiv). The tube was sealed with a rubber septum and taken out of the glove box. 3,11-Dibromo-dibenzo[*a,j*]phenazine (**8**) (40.7 mg, 0.09 mmol), 10,10-diisopropyl-5,10-dihydrodibenzo[b,e][1,4]azasiline (**9**) (57.1 mg, 0.20 mmol, 2.2 equiv), and toluene (5 mL) were added to the tube under a stream of N_2 gas at room temperature, and the resulting mixture was stirred at 80°C for 24 h. Water (15 mL) was added to the reaction mixture, and the organic layer was extracted with $CHCl_3$ (20 mL × 3). The combined organic extracts were dried over Na_2SO_4, and the solvent was evaporated in vacuo to give the crude product, which was purified by flash column chromatography on NH silica gel (eluent: *n*-hexane/ EtOAc 9:1) followed by recrystallization from a two-phase solvent of *n*-hexane/$CHCl_3$, affording the title compound as yellow solid (41.3 mg, 0.05 mmol, 55%). Mp 313 °C (dec.); T_d (5 wt% loss) 440 °C (under N_2); 366 °C (under air); R_f 0.48 (*n*-hexane/EtOAc 8:2, NH silica); ^{1}H NMR (400 MHz, $CDCl_3$): δ 9.90 (d, J = 8.4 Hz, 2H), 8.19 (d, J = 9.2 Hz, 2H), 8.13 (d,

J = 9.6 Hz, 2H), 7.93 (d, *J* = 1.6 Hz, 2H), 7.80 (dd, *J* = 8.4, 1.6 Hz, 2H), 7.61 (dd, *J* = 7.6, 2.0 Hz, 4H), 7.11 (ddd, *J* = 7.6, 7.2, 1.6 Hz, 4H), 6.94 (dd, *J* = 7.2, 7.2 Hz, 4H), 6.41 (d, *J* = 8.4 Hz, 4H), 1.54–1.48 (m, 4H), 1.15 (d, *J* = 7.2 Hz, 24H); ^{13}C NMR (100 MHz, $CDCl_3$): δ 150.4, 145.1, 143.1, 140.5, 135.6, 134.6, 132.3, 131.2, 130.6, 130.4, 129.7, 128.3, 127.8, 119.5, 117.2, 116.0, 18.2, 12.8; ^{29}Si NMR (119 MHz, $CDCl_3$): δ –18.0; IR (ATR): ν 3051, 2941, 2862, 1583, 1568, 1481, 1458, 1425, 1352, 1301, 1240, 1103, 993, 927, 879, 854, 800, 744 cm^{-1}; MS (FAB$^+$, NBA): *m/z* (relative intensity, %) 839 ([M+H]$^+$, 100), 795 ([M–*i*-Pr]$^+$, 62), 753 ([M–2*i*-Pr+H]$^+$, 14), 709 ([M–3*i*-Pr]$^+$, 7), 667 ([M–4*i*-Pr+H]$^+$, 10); HRMS (FAB$^+$, NBA): *m/z* calcd for $C_{56}H_{55}N_4Si_2$ ([M+H]$^+$) 839.3965, found 839.3983. Anal. Calcd for $C_{56}H_{54}N_4Si_2$: C, 80.15; H, 6.49; N, 6.68. Found: C, 80.08; H, 6.69; N, 6.67.

Synthetic procedures for 3,11-di(5H-spiro[dibenzo[b,e][1,4]azasiline-10,10'-dibenzo[b,e][1,4]oxasilin]-5-yl)dibenzo[a,j]phenazine (**3**)

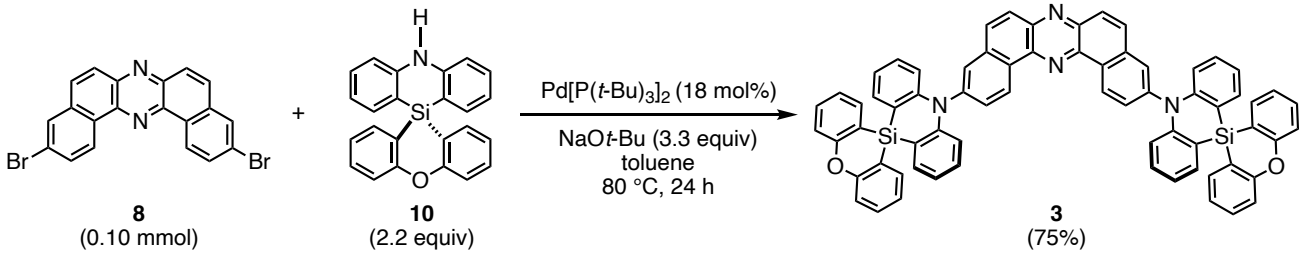

A two-necked reaction tube (10 mL) equipped with a magnetic stir bar was transferred into a glovebox. To the tube, were added Pd[P(*t*-Bu)$_3$]$_2$ (9.0 mg, 17.6 μmol, 18 mol%) and NaO*t*-Bu (30 mg, 0.20 mmol, 2.2 equiv). The tube was sealed with a rubber septum and taken out of the glove box. 3,11-Dibromo-dibenzo[*a,j*]phenazine (**8**) (41.9 mg, 0.10 mmol), **10** (77.6 mg, 0.21 mmol, 2.2 equiv), and toluene (3 mL) were added to the tube under a stream of N_2 gas at room temperature, and the resulting mixture was stirred at 80 °C for 24 h. Water (5 mL) was added to the reaction mixture, and the organic layer was extracted with $CHCl_3$ (20 mL × 3). The combined organic extracts were dried over Na_2SO_4, and the solvent was evaporated in vacuo to give the crude product, which was purified by flash column chromatography on NH silica gel (eluent: *n*-hexane/EtOAc 8:2) followed by recrystallization from a two-phase solvent of *n*-hexane/$CHCl_3$, affording the title compound **3** as yellow solid (72.1 mg, 0.07 mmol, 75%). Mp >400 °C (dec.); T_d (5 wt% loss) 490 °C (under N_2); 495 °C (under air); R_f 0.18 (*n*-hexane/EtOAc 8:2, NH silica); ^{1}H NMR (400 MHz, $CDCl_3$): δ 10.02 (d, *J* = 8.4 Hz, 2H), 8.27 (d, *J* = 9.2 Hz, 2H), 8.24 (d, *J* = 9.2 Hz, 2H), 8.12 (d, *J* = 2.0 Hz, 2H), 7.96 (dd, *J* = 8.8, 2.0 Hz, 2H), 7.52–7.48 (m, 8H), 7.38 (dd, *J* = 7.2, 2.0 Hz, 4H), 7.35 (d, *J* = 8.0 Hz, 4H), 7.19–7.11 (m, 8H), 6.88 (dd, *J* = 7.0, 7.0 Hz, 4H), 6.53 (d, *J* = 9.2 Hz, 4H); ^{13}C NMR (100 MHz, $CDCl_3$): δ 160.9, 150.4, 144.6, 143.4, 140.6, 136.8, 136.2, 135.8, 132.3, 132.2, 131.81, 131.79, 131.0, 130.8, 128.6, 128.2, 122.9, 120.3, 117.9, 117.6, 117.2, 115.7; ^{29}Si NMR (119 MHz, $CDCl_3$): δ –49.6; IR (ATR): ν 3059, 3001, 1585, 1568, 1458, 1421, 1303, 1265, 1215, 1126, 1090, 1074, 885, 808, 748 cm^{-1}; MS (FAB$^+$, NBA): *m/z* (relative intensity, %) 1003 ([M+H]$^+$, 10), 1002 (M$^+$, 7); HRMS (FAB$^+$, NBA): *m/z* calcd for $C_{68}H_{43}N_4O_2Si_2$ ([M+H]$^+$) 1003.2925, found 1003.2942. Anal. Calcd for $C_{68}H_{42}N_4O_2Si_2$: C, 81.41; H,

4.22; N, 5.58. Found: C, 81.12; H, 4.50; N, 5.62.

Synthetic procedures for 2,12-bis(10,10-diphenyldibenzo[b,e][1,4]azasilin-5(10H)-yl)dibenzo[a,j]phenazine (**4**)

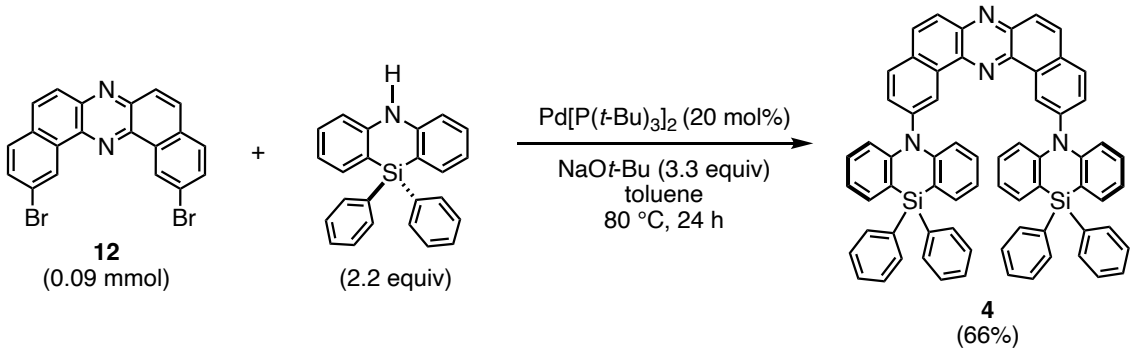

A two-necked reaction tube (10 mL) equipped with a magnetic stir bar was transferred into a globe box. To the tube, were added Pd[P(*t*-Bu)$_3$]$_2$ (9.0 mg, 0.02 mmol, 20 mol%) and NaO*t*-Bu (30 mg, 0.30 mmol, 3.3 equiv). The tube was sealed with a rubber septum and taken out the glove box. 2,12-Dibromo-dibenzo[*a,j*]phenazine (**12**) (40.6 mg, 0.09 mmol), 10,10-diphenyl-5,10-dihydrodibenzo[*b*,*e*][1,4]azasiline (72.0 mg, 0.21 mmol, 2.2 equiv) and toluene (5 mL) were added to the tube under a stream of N_2 gas at room temperature, and the resulting mixture was stirred at 80 °C for 24 h. Water (15 mL) was added to the reaction mixture, and the organic layer was extracted with $CHCl_3$ (20 mL × 3). The combined organic extracts were dried over Na_2SO_4, and the solvent was evaporated in vacuo to give the crude product, which was purified by flash column chromatography on NH silica gel (eluent: *n*-hexane/$CHCl_3$ 8:2) followed by recrystallization from a two-phase solvent of *n*-hexane/$CHCl_3$, affording the title compound **4** as orange solid (59.8 mg, 0.06 mmol, 66%). Mp 343 °C (dec.); T_d (5 wt% loss) 451 °C (under N_2); 448 °C (under air); R_f 0.20 (*n*-hexane/ EtOAc 8:2, NH silica); ^{1}H NMR (400 MHz, CD_2Cl_2): δ 9.49 (d, J = 2.0 Hz, 2H), 8.27 (s, 4H), 8.22 (d, J = 8.0 Hz, 2H), 7.54–7.60 (m, 14H), 7.26–7.33 (m, 12H), 7.08 (ddd, J = 7.8, 7.8, 1.8 Hz, 4H), 6.88 (dd, J = 7.6, 7.6 Hz, 4H), 6.56 (d, J = 8.8 Hz, 4H); ^{13}C NMR (100 MHz, $CDCl_3$): δ 150.0, 143.5, 143.2, 140.5, 136.1, 135.8, 135.0, 132.9, 132.5, 132.3, 131.8, 131.71, 131.66, 130.4, 129.6, 127.9, 127.6, 120.4, 118.4, 117.0; ^{29}Si NMR (119 MHz, $CDCl_3$): δ –32.0; IR (ATR): ν 3047, 3003, 1608, 1582, 1564, 1516, 1456, 1427, 1352, 1301, 1232, 1103, 934, 829, 756 cm^{-1}; MS (FAB$^+$, NBA): *m/z* (relative intensity, %) 975 ([M+H]$^+$, 42), 897 ([M–Ph]$^+$, 8), 820 ([M–2Ph]$^+$, 2); HRMS (FAB$^+$, NBA): *m/z* calcd for $C_{68}H_{46}N_4Si_2$ (M^+) 974.3261, found 974.3248; Anal. Calcd for $C_{68}H_{46}N_4Si_2$: C, 83.74; H, 4.75; N, 5.74. Found: C, 84.02; H, 5.10; N, 5.76.

Synthetic procedures for 2,12-bis(10,10-diisopropyldibenzo[b,e][1,4]azasilin-5(10H)-yl)dibenzo[a,j]phenazine (**5**)

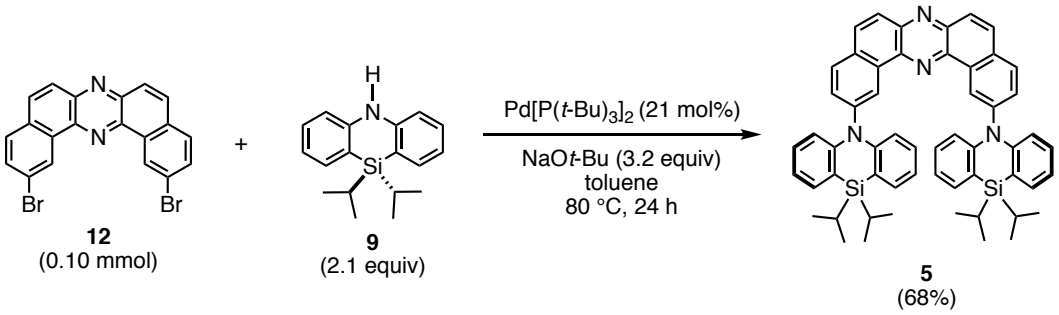

A two-necked reaction tube (10 mL) equipped with a magnetic stir bar was transferred into a glove box. To the tube, were added Pd[P(*t*-Bu)$_3$]$_2$ (9.0 mg, 0.02 mmol, 21 mol%) and NaO*t*-Bu (30 mg, 0.31 mmol, 3.2 equiv). The tube was sealed with a rubber septum and taken out of the glove box. 2,12-Dibromo-dibenzo[*a,j*]phenazine (**12**) (42.2 mg, 0.10 mmol), **9** (57.9 mg, 0.21 mmol, 2.1 equiv) and toluene (5 mL) were added to the tube under a stream of N_2 gas at room temperature, and the resulting mixture was stirred at 80°C for 24 h. Water (15 mL) was added to the reaction mixture, and the organic layer was extracted with $CHCl_3$ (20 mL × 3). The combined organic extracts were dried over Na_2SO_4, and the solvent was evaporated in vacuo to give the crude product, which was purified by flash column chromatography on NH silica gel (eluent: *n*-hexane/$CHCl_3$ 8:2) followed by recrystallization from a two-phase solvent of *n*-hexane/$CHCl_3$, affording the title compound **5** as yellow solid (55.0 mg, 0.07 mmol, 68%). Mp 347 °C (dec.); T_d (5 wt% loss) 297 °C (under N_2); 332 °C (under air); R_f 0.31 (*n*-hexane/EtOAc 8:2, NH silica); ^{1}H NMR (400 MHz, $CDCl_3$): δ 9.33 (d, J = 2.0 Hz, 2H), 8.22–8.16 (m, 6H), 7.62 (dd, J = 8.4, 2.0 Hz, 2H), 7.51 (dd, J = 7.6, 1.8 Hz, 4H), 7.00 (ddd, J = 8.0, 7.8, 1.6 Hz, 4H), 6.84 (ddd, J = 7.6, 6.8, 0.8 Hz, 4H), 6.40 (d, J = 8.8 Hz, 4H), 1.42–1.32 (m, 4H), 1.02 (d, J = 7.2 Hz, 24H); ^{13}C NMR (100 MHz, $CDCl_3$): δ 150.5, 143.8, 143.1, 140.3, 134.4, 133.3, 132.6, 132.5, 132.2, 131.1, 129.7, 127.9, 127.6, 119.5, 117.8, 116.5, 18.0, 12.6; ^{29}Si NMR (119 MHz, $CDCl_3$): δ –17.9; IR (ATR): ν 3007, 2918, 2891, 1583, 1458, 1427, 1305, 1234, 1192, 1166, 1103, 939, 881, 846, 746 cm^{-1}; MS (FAB$^+$, NBA): *m/z* (relative intensity, %) 839 ([M+H]$^+$, 100), 795 ([M–*i*-Pr]$^+$, 11), 753 ([M–2*i*-Pr+H]$^+$, 13), 710 ([M–3*i*-Pr+H]$^+$, 7), 667 ([M–4*i*-Pr+H]$^+$, 10); HRMS (FAB$^+$, NBA): *m/z* calcd for $C_{56}H_{55}N_4Si_2$ ([M+H]$^+$) 839.3965, found 839.3952. Anal. Calcd for $C_{56}H_{54}N_4Si_2$: C, 80.15; H, 6.49; N, 6.68. Found: C, 80.20; H, 6.66; N, 6.64.

Synthetic procedures for 2,12-di(5H-spiro[dibenzo[b,e][1,4]azasiline-10,10'-dibenzo[b,e][1,4]oxasilin]-5-yl)dibenzo[a,j]phenazine (**6**)

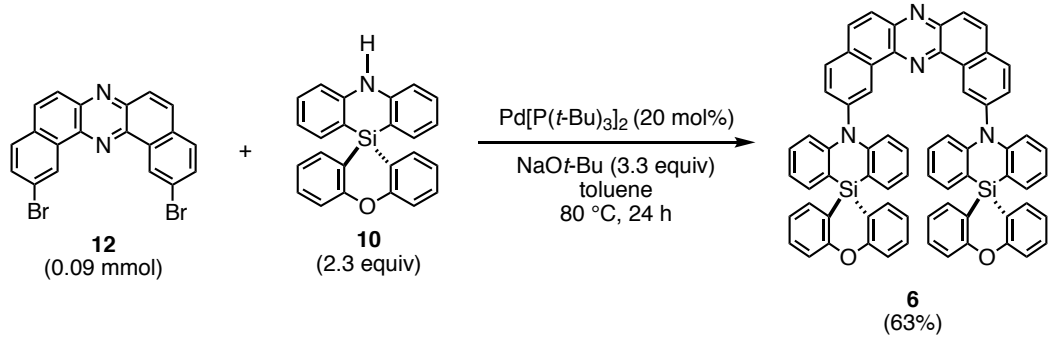

A two-necked reaction tube (10 mL) equipped with a magnetic stir bar was transferred into a glove box. To the tube, were added $Pd[P(t\text{-}Bu)_3]_2$ (9.0 mg, 0.02 mmol, 20 mol%) and NaO*t*-Bu (30 mg, 0.30 mmol, 3.3 equiv). The tube was sealed with a rubber septum and taken out of the glove box. 2,12-Dibromo-dibenzo[*a,j*]phenazine (**12**) (40.0 mg, 0.09 mmol), **10** (76.7 mg, 0.21 mmol, 2.3 equiv) and toluene (5 mL) were added to the tube under a stream of N_2 gas at room temperature, and the resulting mixture was stirred at 80 °C for 24 h. Water (15 mL) was added to the reaction mixture, and the organic layer was extracted with $CHCl_3$ (20 mL × 3). The combined organic extracts were dried over Na_2SO_4, and the solvent was evaporated in vacuo to give the crude product, which was purified by flash column chromatography on NH silica gel (eluent: *n*-hexane/$CHCl_3$ 8:2) followed by recrystallization from a two-phase solvent of *n*-hexane/$CHCl_3$, affording the title compound **6** as yellow solid (57.9 mg, 0.06 mmol, 63%). Mp 397 °C (dec.); T_d (5 wt% loss) = 483 °C (under N_2); 425 °C (under air); R_f 0.53 (*n*-hexane/EtOAc 6:4, NH silica); ^{1}H NMR (400 MHz, $CDCl_3$): δ 9.65 (d, J = 2.0 Hz, 2H), 8.44–8.38 (m, 6H), 7.81 (dd, J = 8.4, 2.0 Hz, 2H), 7.37 (ddd, J = 8.8, 6.6, 1.8 Hz, 4H), 7.33–7.27 (m, 12H), 7.80 (ddd, J = 8.2, 8.2, 2.0 Hz, 4H), 6.83–6.78 (m, 8H), 6.54 (d, J = 8.8 Hz, 2H); ^{13}C NMR (100 MHz, $CDCl_3$): δ 160.7, 150.4, 143.3, 143.0, 136.6, 136.3, 133.0, 132.4, 132.3, 131.8, 130.8, 128.04, 128.03, 128.00, 122.8, 120.3, 117.65, 117.64, 117.5, 117.2, 117.2, 116.0; ^{29}Si NMR (119 MHz, $CDCl_3$): δ –49.7; IR (ATR): ν 3051, 3003, 1585, 1568, 1460, 1421, 1301, 1263, 1215, 1126, 1074, 931, 883, 844, 795, 748 cm^{-1}; MS (FAB^+, NBA): *m/z* (relative intensity, %) 1003 ($[M+H]^+$, 31), 1002 (M^+, 25); HRMS (FAB^+, NBA): *m/z* calcd for $C_{68}H_{42}N_4O_2Si_2$ (M^+) 1002.2846, found 1002.2868. Anal. Calcd for $C_{68}H_{42}N_4O_2Si_2$: C, 81.41; H, 4.22; N, 5.58. Found: C, 81.52; H, 4.30; N, 5.60.

Single Crystal X-Ray Crystallographic Analysis.

Crystallographic analysis of compound **3**: The single crystal suitable for the X-ray crystallographic analysis was grown from a biphasic solution of *n*-hexane/$CHCl_3$ by slow evaporation. XtaLAB P200 diffractometer with graphite monochromated CuKα radiation (λ = 1.54187 Å) to a $2\theta_{max}$ value of 149.1° at 213 K. The cell refinements were performed with a software CrysAlisPro 1.171.39.5a.[S5] The crystal structure was solved by direct methods (SHELXT Version 2014/5).[S6] All calculations were performed with the observed reflections [I > 2σ(I)] with the program CrystalStructure crystallographic software packages,[S7] except for refinement which was performed by SHELXL.[S8] The non-hydrogen atoms were refined anisotropically, and hydrogen atoms were refined using the riding model. The crystal data are summarized in Table SX. CCDC-2121902 contains the supplementary crystallographic data for **3**, which are available free of charge from the Cambridge Crystallographic Data Center (CCDC) via www.ccdc.cam.ac.uk/data_request/cif.

Crystallographic analysis of compound **6**: The single crystal suitable for the X-ray crystallographic analysis was grown from a biphasic solution of *n*-hexane/$CHCl_3$ by slow evaporation. XtaLAB P200 diffractometer with graphite monochromated CuKα radiation (λ = 1.54187 Å) to a $2\theta_{max}$ value of 149.3° at 213 K. The cell refinements were performed with a software CrysAlisPro 1.171.39.5a.[S5] The crystal structure was solved by direct methods (SHELXT Version 2014/5).[S6] All calculations were performed with the observed reflections [I > 2σ(I)] with the program Olex2 (1.2) platform,[S9] except for refinement which was performed by SHELXL.[S8] The non-hydrogen atoms were refined anisotropically, and hydrogen atoms were refined using the riding model. The crystal data are summarized in Table S2. CCDC-2121903 contains the supplementary crystallographic data for **6**, which are available free of charge from the Cambridge Crystallographic Data Center (CCDC) via www.ccdc.cam.ac.uk/data_request/cif.

Table S1. Summary of the crystallographic data of compound **3**.

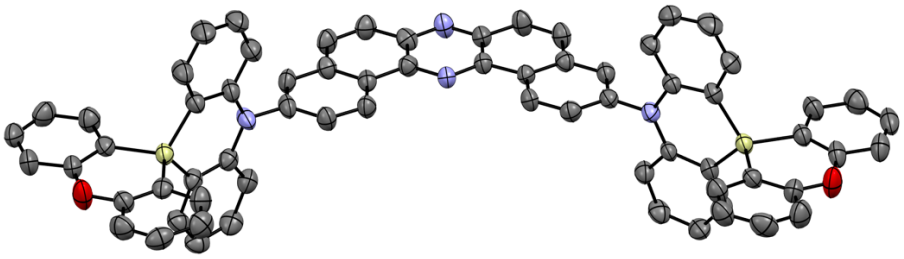

Empirical Formula	$C_{68}H_{42}N_4O_2Si_2$ + solvent	
Formula Weight	1003.28	
Crystal System	monoclinic	
Space Group	C2/c (#15)	
Unit cell dimensions	a = 33.5551(7) Å	α = 90°
	b = 9.0237(2) Å	β = 93.5378(18)°
	c = 46.7263(7) Å	γ = 90°
V	14121.4(5) Å^3	
Z	8	
Density (calculated)	0.944 g/cm^3	
Absorption coefficient	7.58 cm^{-1}	
R_1 [I>2σ(I)]	0.1230	
wR_2 (all data)	0.3878	
Crystal size	0.200 × 0.010 × 0.010 mm	
Goodness-of-fit on F^2	0.974	
Reflections collected/unique	13870/9970 [R(int) = 0.0461]	

Table S2. Summary of the crystallographic data of compound **6**.

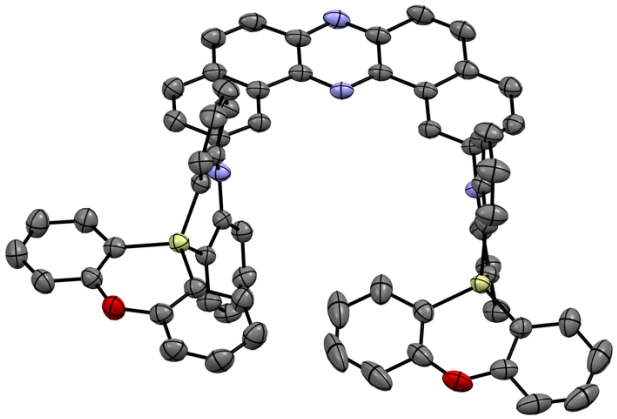

Empirical Formula	$C_{68}H_{42}N_4O_2Si_2$ + solvent	
Formula Weight	1003.28	
Crystal System	triclinic	
Space Group	P–1 (#2)	
Unit cell dimensions	a = 11.3988(2) Å	α = 78.830(1)°
	b = 13.8638(2) Å	β = 85.484(1)°
	c = 21.0832(3) Å	γ = 70.838(1)°
V	3087.16(9) Å^3	
Z	2	
Density (calculated)	1.079 g/cm^3	
Absorption coefficient	8.67 cm^{-1}	
R_1 [I>2σ(I)]	0.0412	
wR_2 (all data)	0.1185	
Crystal size	0.200 × 0.200 × 0.030 mm	
Goodness-of-fit on F^2	1.061	
Reflections collected/unique	12187/10263 [R(int) = 0.0355]	

UV-vis Absorption and PL Spectra of Compounds 2, 3, 5, and 6

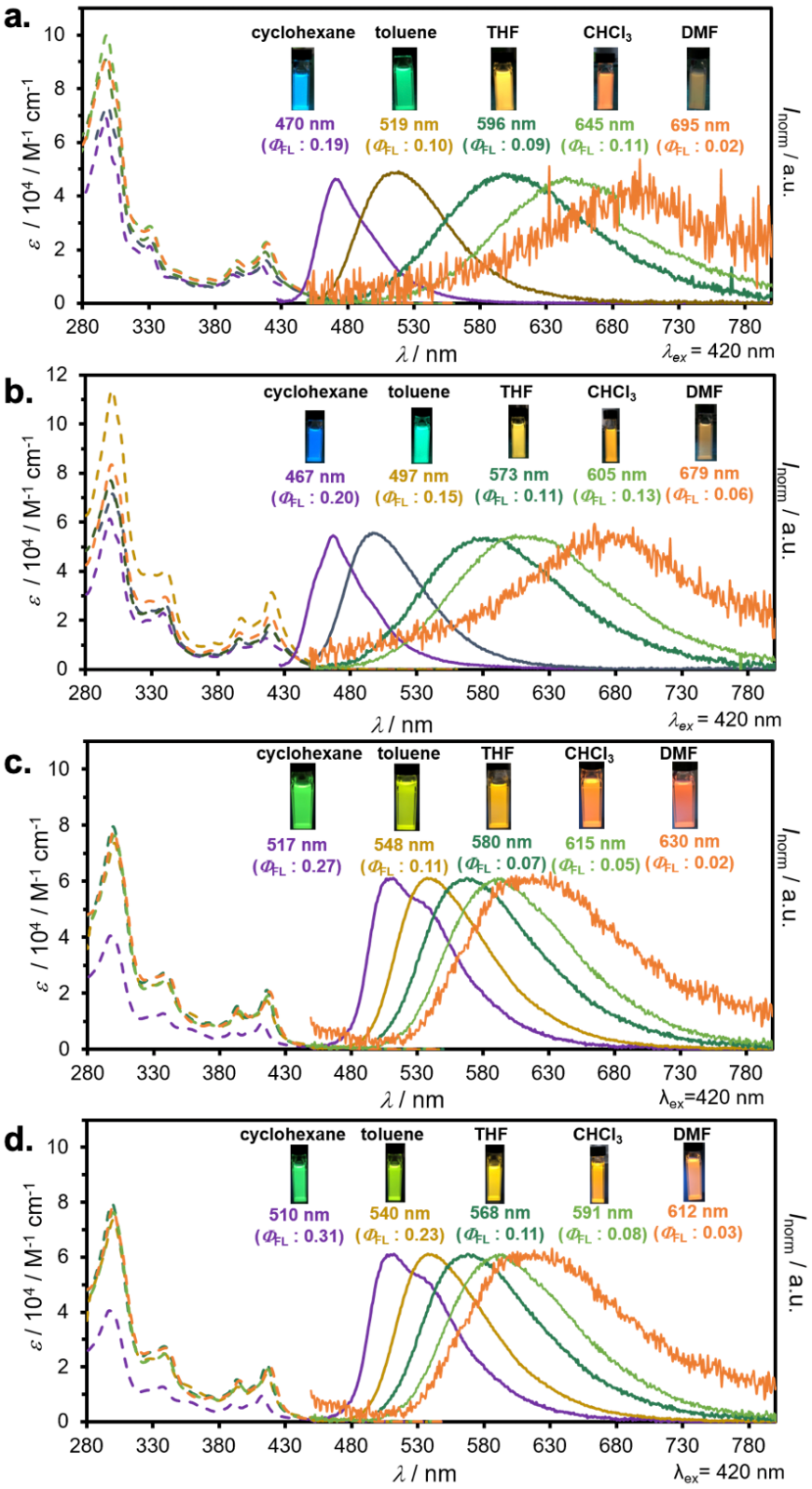

Fig. S1 UV-vis absorption and PL spectra of diluted solutions of a) **2**, b) **3**, c) **5**, and d) **6** (c 10^{-5} M).

Additional Photophysical Results

Time-resolved measurements were performed by exponentially increasing the gate and delay times of iCCD Stanford Computer Optics 4Picos camera from laser excitation. The delay and integration times are set at a time longer than the previous sum of delay and integration time to avoid overlap. As the next step, the curve is corrected by integrating the measured spectra to obtain proper luminescence decay profile. Every point represents the collected emission spectra of respective emitting specie.

To understand the actual recombination processes involved in the light generation, more detailed photophysical studies were conducted (Fig. S2 and Fig. S3). The photofunctional parameters are summarized in Table 1. The analysis revealed the influence caused by not only molecular structure but also host material on the observed emission processes. Depending on the combination of the molecular structure and host material, TADF, RTP, dual TADF & RTP, or dual RTP from the T_1 and T_2 states were observed (Fig. S2). As the analysis of emission change after the excitation with laser, the PL emission intensity versus a particular delay time in Zeonex® matrix showed emissions associated with dual TADF & RTP processes for all the compounds (Fig. S2a–e). The transient intensity curves displayed a classical behavior of TADF and RTP process for compounds **2**, **3**, **5** and **6**, where the delay component in μs delay region increased as a function of temperature (TADF process), and the component in ms delay region decreased as a function of temperature (phosphorescence process). It should be noted that the long delayed component (phosphorescence) was not technically observed for compound 2,12-regioisomer **4**, probably due to the overlap with long-lived TADF emission. Nevertheless, only the compound **3** based on 3,11-substituted D–A–D scaffold showed significant contributions of RTP emission (>50%, Fig. S2b and S3b). In the case of compounds **2** and **6**, the RTP contribution is above 1% (Fig. S3a, e) and lower than 1% for compounds **4** and **5** (Fig. S3c, d).

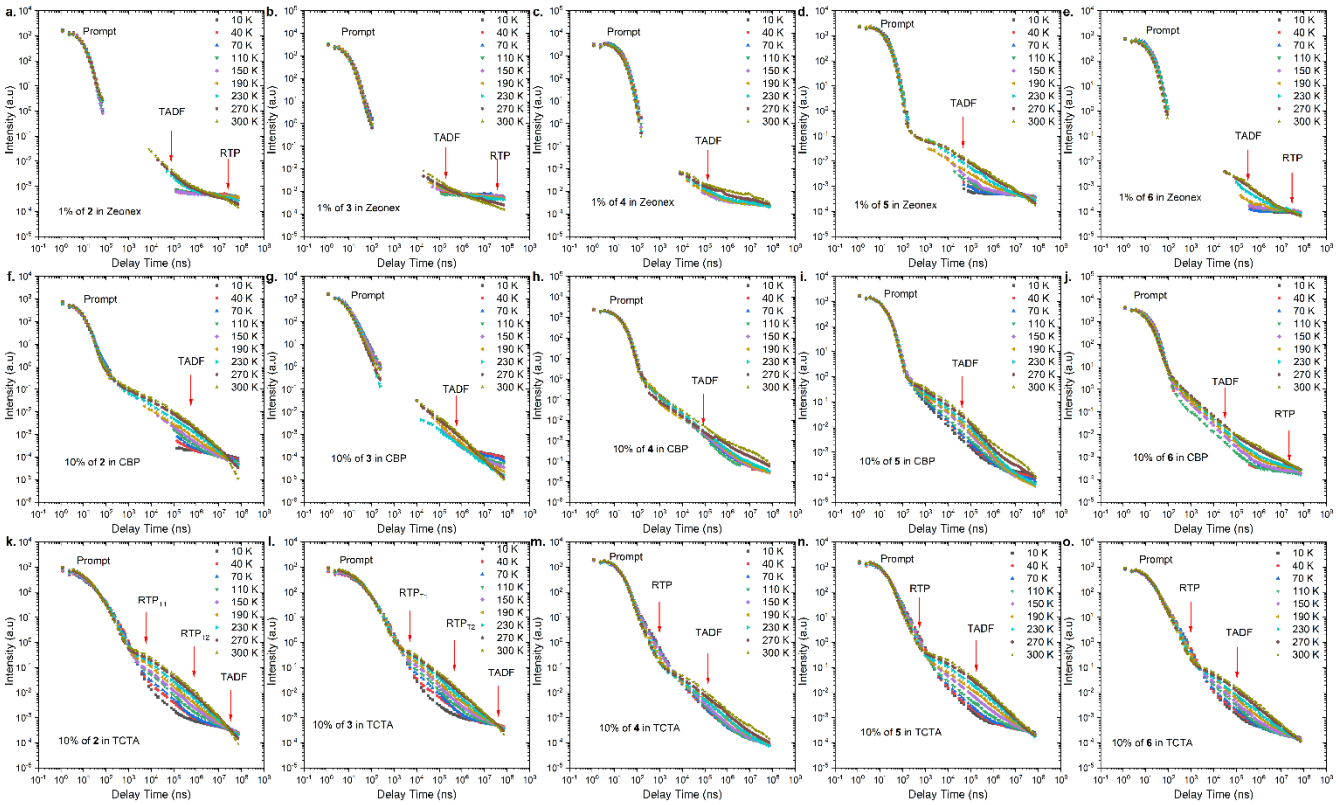

Fig. S2 Photophysical properties of compounds **2**−**6** in a different matrix. Intensity vs. delay time at different temperatures in various hosts. a) **2**, b) **3**, c) **4**, d) **5**, and e) **6** (1 wt%) in Zeonex®; f) **2**, g) **3**, h) **4**, i) **5**, and j) **6** (10 wt%) in CBP; k) **2**, l) **3**, m) **4**, n) **5**, and o) **6** (10 wt%) in TCTA host.

For the purpose of application study, further time-resolved spectroscopic analysis in an OLED host was conducted (Fig. S2 f–o, and S3f–o). Based on our previous study, we compared the behavior of the emitters in CBP [4,4′-bis(*N*-carbazolyl)-1,1′-biphenyl] and TCTA [4,4',4"-tri(9-carbazoyl)triphenylamine] matrix. In the case of behavior in CBP host, all the emitters except for **6** exhibited TADF emission at 300 K (Fig. S2f–i and Fig. S3f–i). The emission intensity *versus* delay time curves of compounds **2**–**5** changed with temperature in the way that delay component related with TADF process increased as a function of temperature whereas the phosphorescence in ms delay regime decreased and disappeared above 150 K (Figure S2f–i). The emission spectra at 300 K for compounds **2**–**5** at the delay time of 70 ms are nicely overlapped with the prompt emission and significantly different from the phosphorescence spectra, indicating the emission of **2**–**5** in CBP is radiated from the S_1 state. In all the cases, the emission spectra are not well-resolved (i.e., Gaussian shape), suggesting the S_1 state is ascribed to ^{1}CT state (Figure S3f–i). It is noted that a different type of emission was observed for 2,12-regioisomeic spiro compound **6**. At a very long delay time, mixed emission of TADF and RTP processes were observed (Figure S3j).

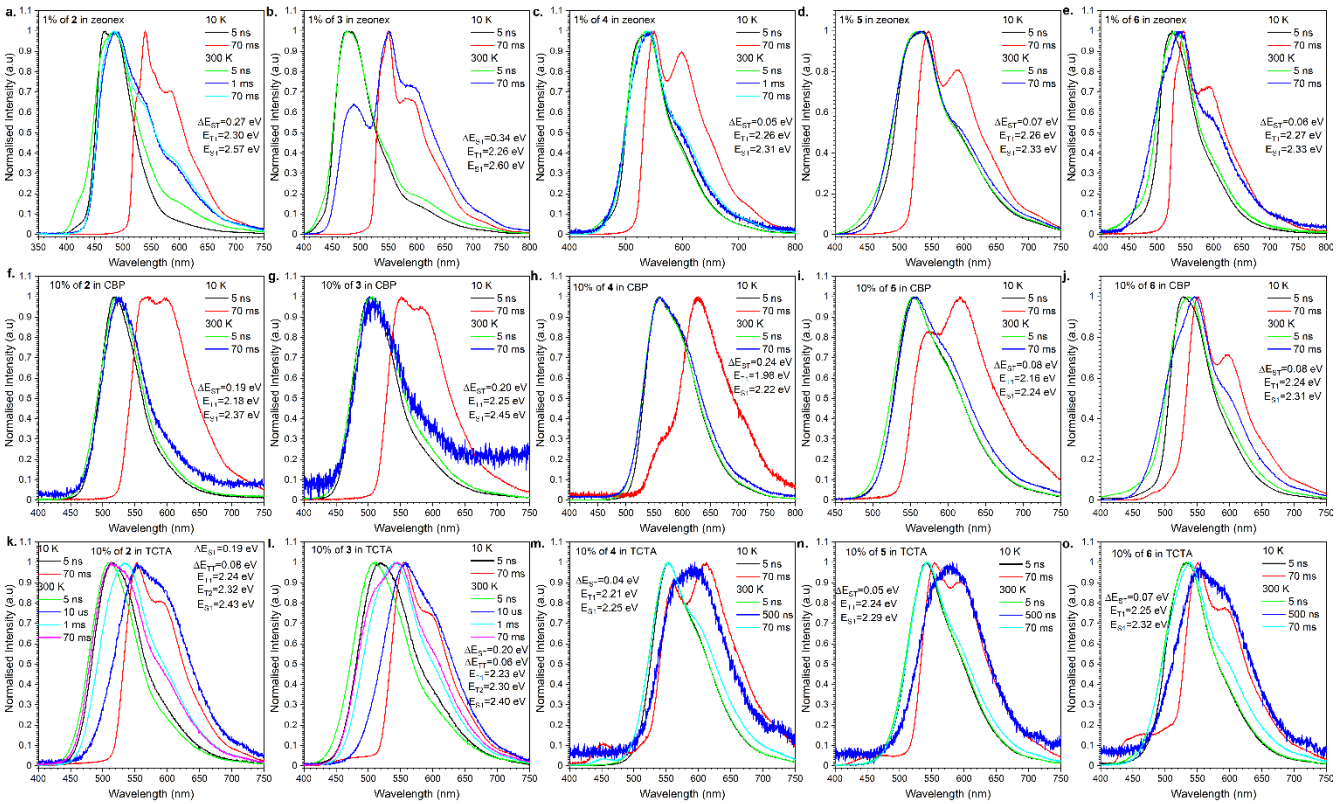

Fig. S3 Time-Resolved Spectra of compounds **2**–**6** in different matrix obtained during the intensity vs. delay time measurement (Fig. 4). The energies correspond to the maximum emission peaks. a) **2**, b) **3**, c) **4**, d) **5**, and e) **6** (1 wt%) in Zeonex®; f) **2**, g) **3**, h) **4**, i) **5**, and j) **6** (10 wt%) in CBP; k) **2**, l) **3**, m) **4**, n) **5**, and o) **6** (10 wt%) in TCTA host.

Most importantly, unusual behavior was observed in TCTA matrix (Fig. S2k–o and Fig. S3k–o). The 3,11-regioisomers **2** and **3** exhibited dual RTP emissions radiated from the T_1 and T_2 states, which are quite short-lived (in µs order) as for phosphorescence (Fig. S2k, l, and Table 1). Also, TADF occurred, but at very long delay times (Fig. S3k,l, Fig. S4). In contrast, the 2,12-regioisomers compounds **4**–**6** displayed dual TADF & RTP emissions, but again surprisingly the RTP is much shorter-lived than TADF (Fig. S2m, n, o, and Table 1). It seems that the RTP occurs below 1 µs, and thus, we observed the decrease of phosphorescence with the increase of temperature (Fig. S2m, n, and o). The shape of the delayed emission spectra corresponds to those acquired at a low temperature at 70 ms delayed phosphorescence (Fig. S5). The TADF emissions for compounds **4**–**6** (2,12-regioisomer) started to be visible after 10 µs delay time and are long-lived, probably due to the extensive ISC/rISC cycling (Fig. S3m, n, o).

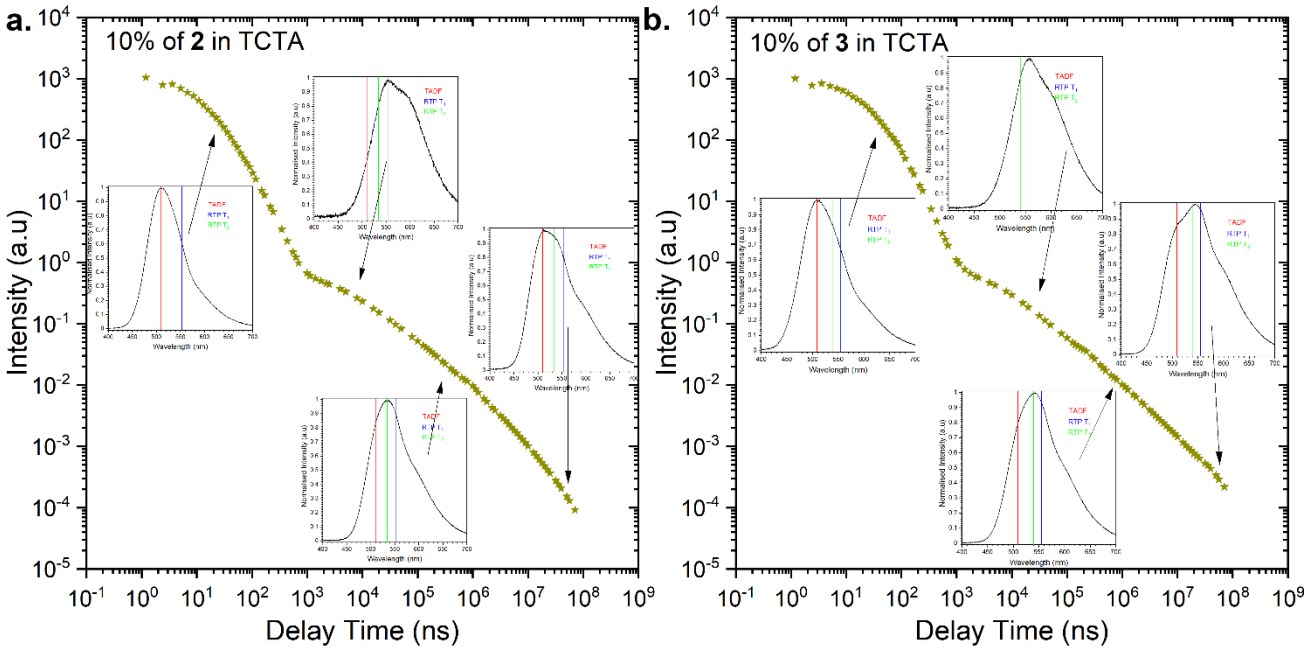

Fig. S4 Photophysical properties of **2** and **3** in TCTA at 300K. (a) Intensity versus delay time of 10% w/w **2** in TCTA. (b) Intensity versus delay time of 10% w/w **3** in TCTA.

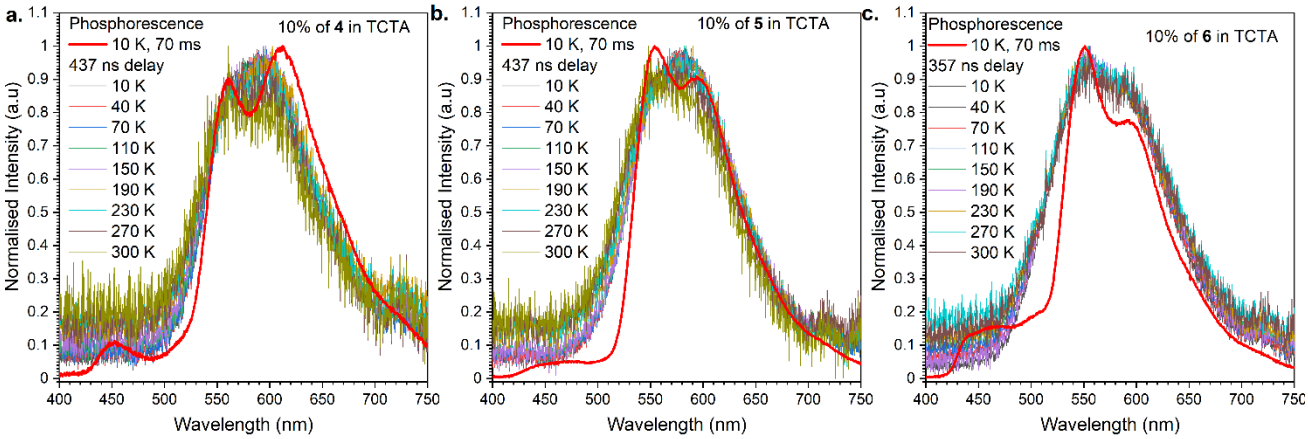

Fig. S5 Time-resolved emissions spectra of **4**, **5**, and **6** in TCTA at various temperature. Comparison of variation of spectra with increase of the temperature and correlation to the phosphorescence emission.

Thermogravimetric Analysis (TGA)

The TGA profiles of **2**–**6** were obtained using a Pt pan under the air or the N_2 gas flow (200 mL/min), starting from 40 °C to 1000 °C at the ramp rate of 10 °C/min.

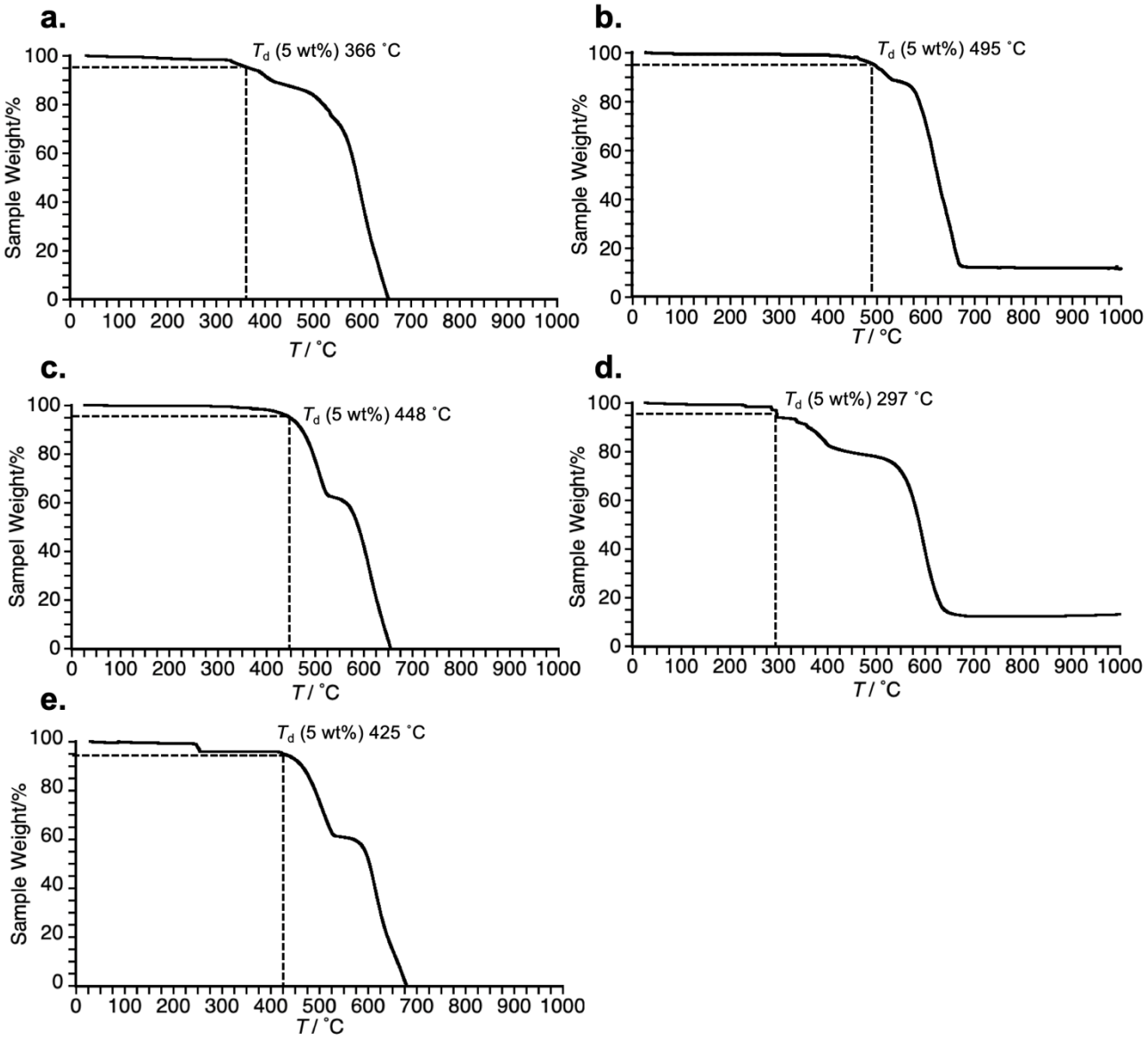

Fig. S6 TGA profiles of a) **2**, b) **3**, c) **4**, d), **5**, and e) **6** under the air.

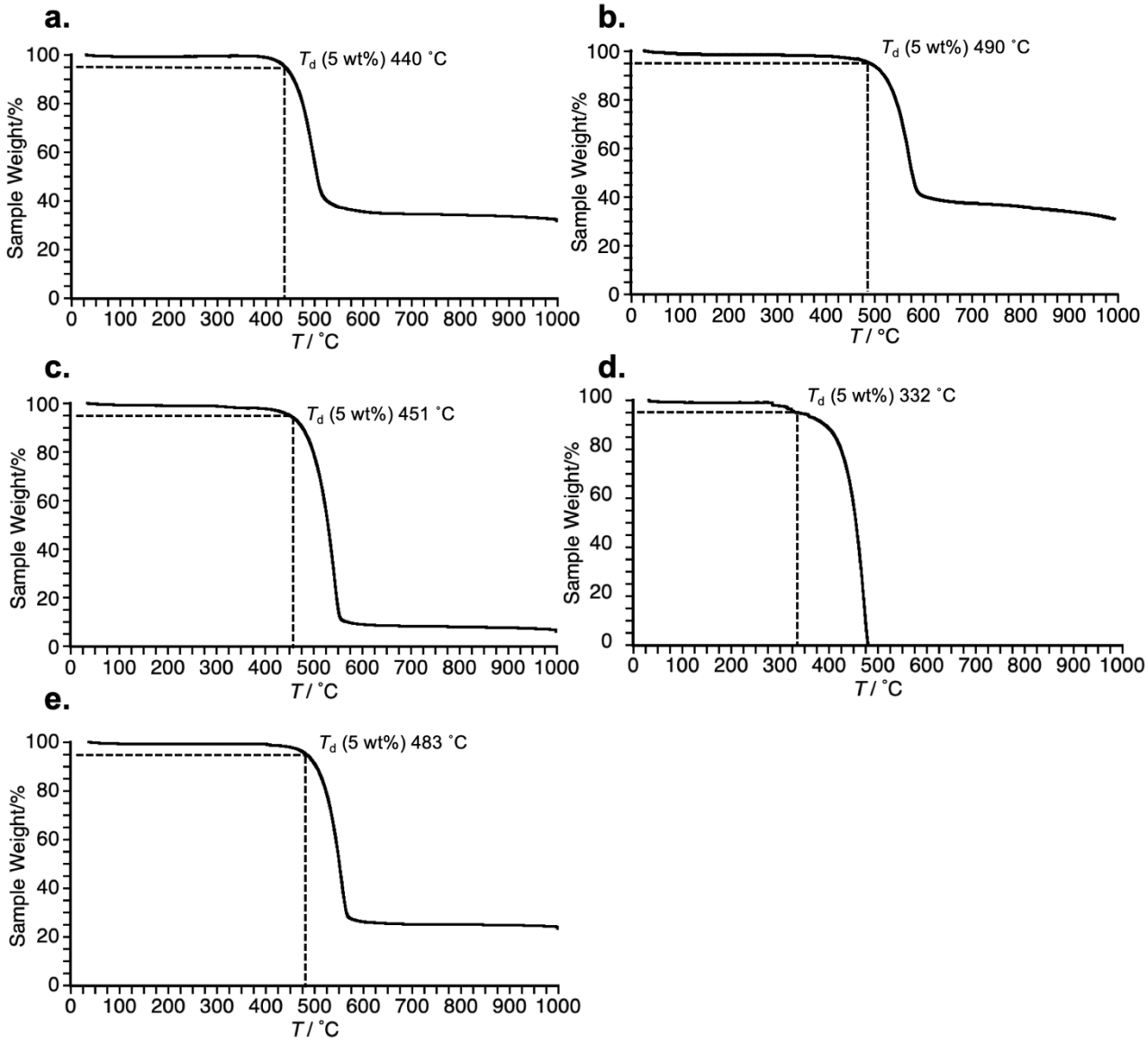

Fig. S7 TGA profiles of a) **2**, b) **3**, c) **4**, d), **5**, and e) **6** under N_2 gas flow.

Cyclic Voltammetry

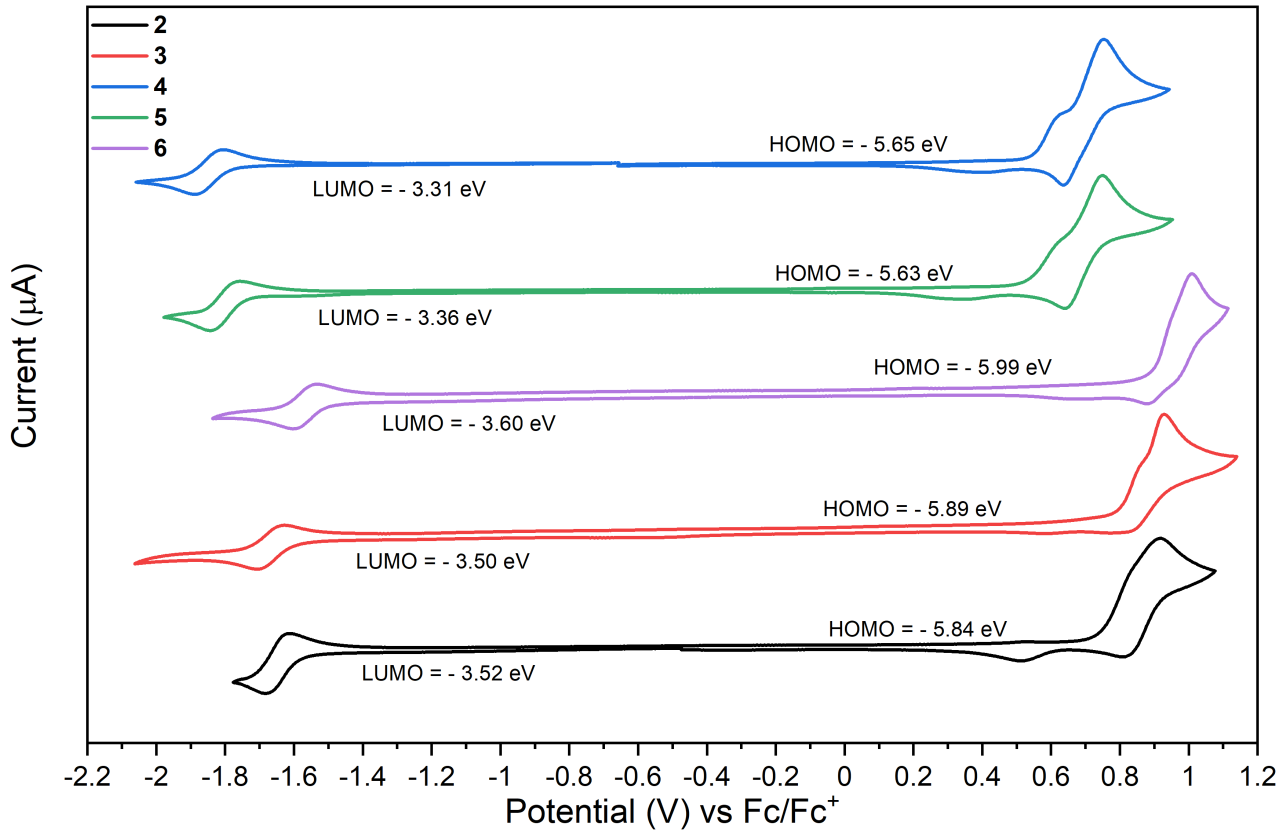

Fig. S8 CV of 1 mM of emitters in 0.1 M Bu_4NBF_4 in DCM electrolyte at the scan rate of 50 mV/s.

OLED Fabrication and Characterization.

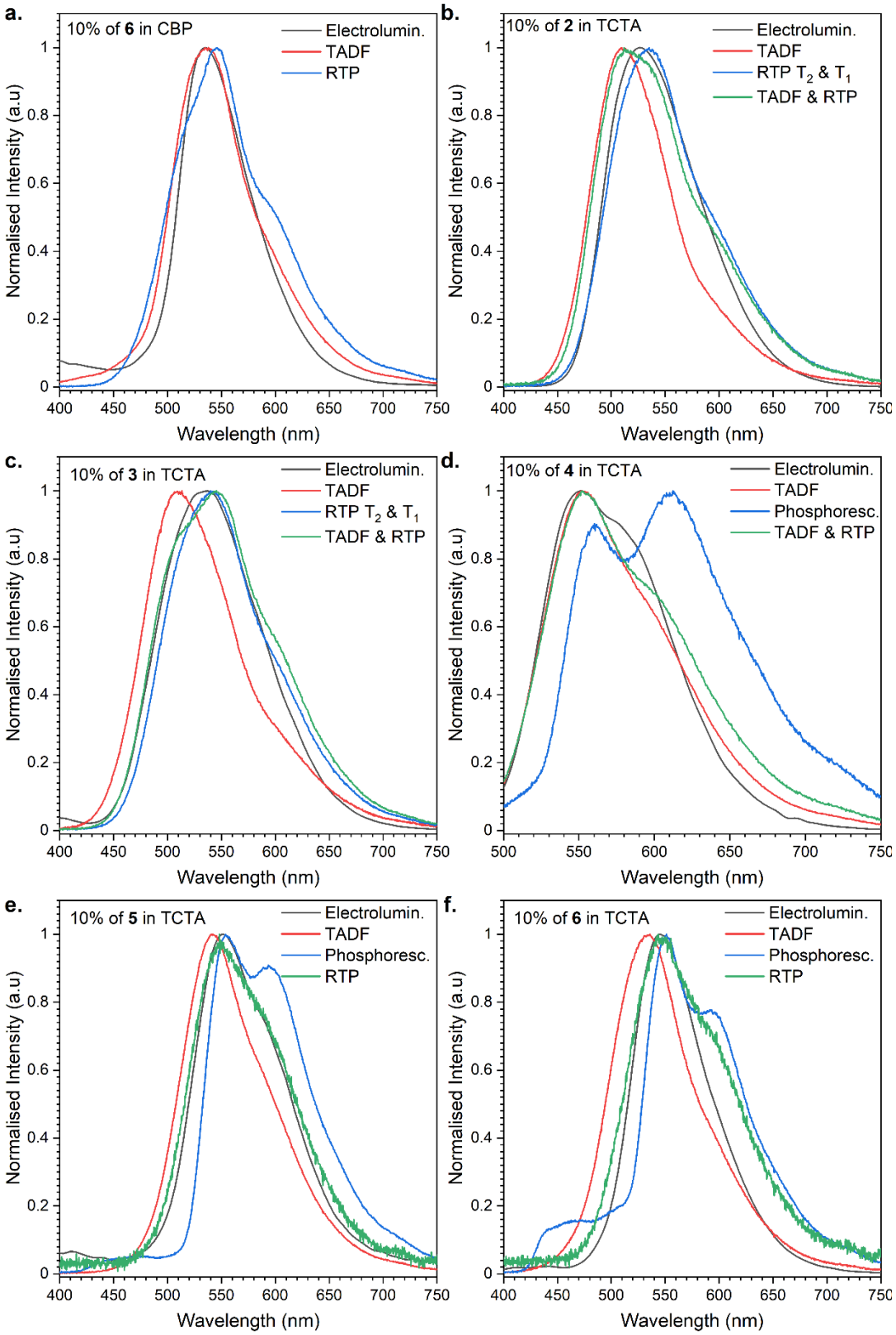

Fig. S9 Comparison of electroluminescence spectra with time-resolved one presenting the respective TADF/RTP processes as components of the emission.

Copies of NMR Charts.

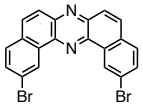

12

^{1}H NMR (400 MHz, $CDCl_3$)

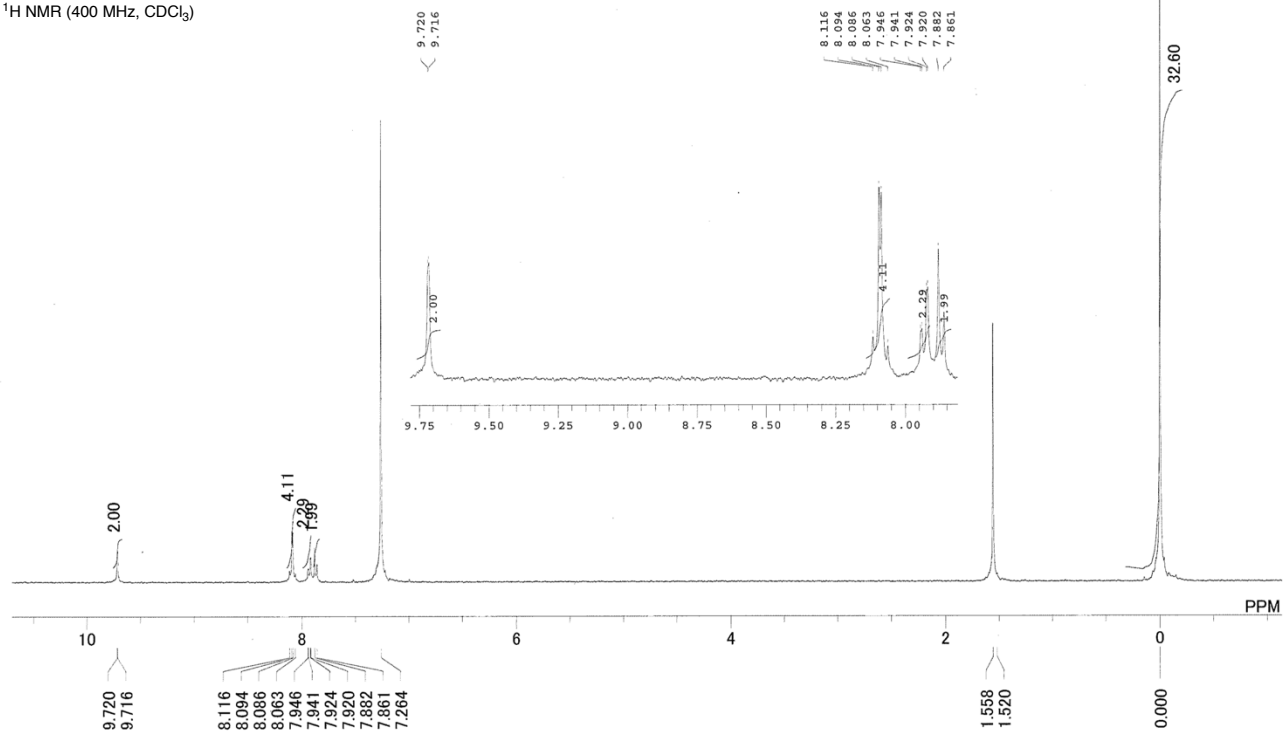

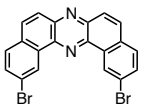

12

^{13}C NMR (100 MHz, $CDCl_3$)

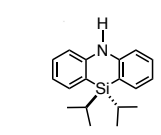

9

^{1}H NMR (400 MHz, $CDCl_3$)

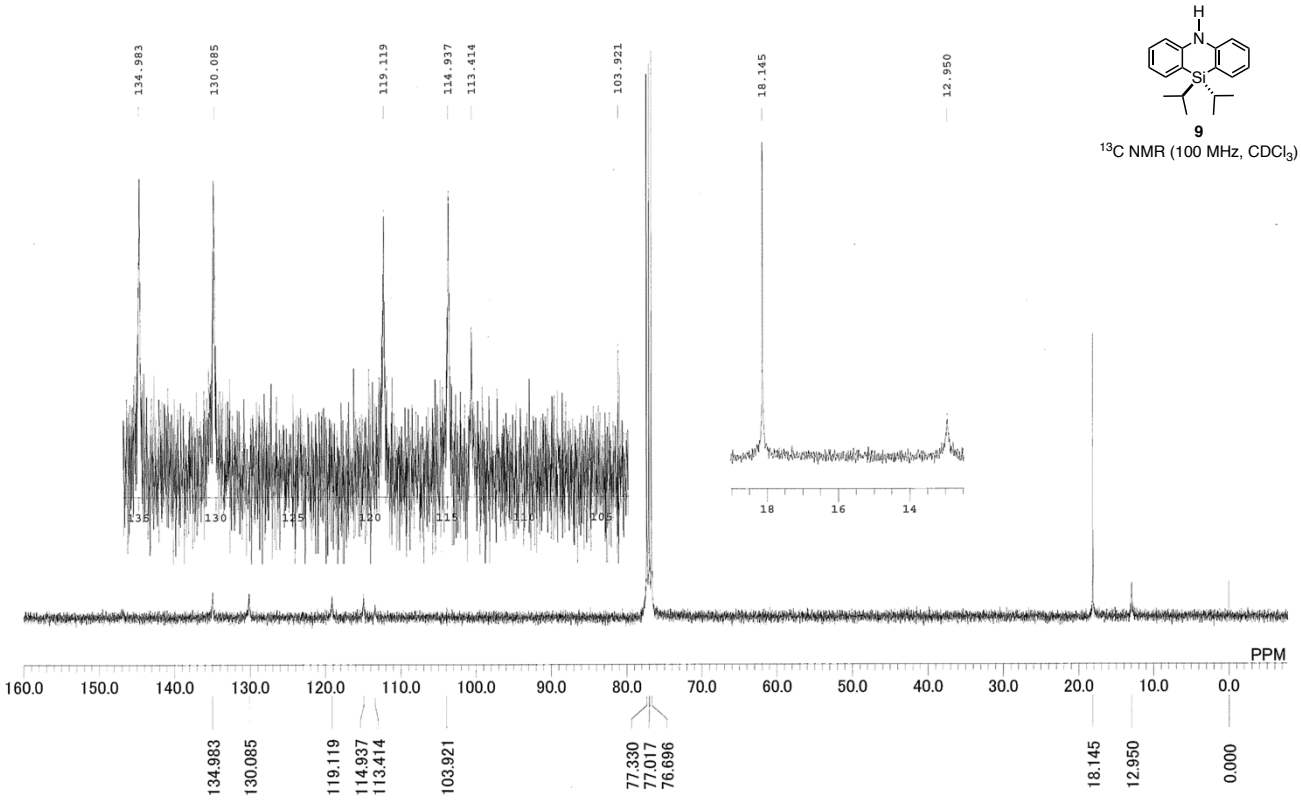

9

^{13}C NMR (100 MHz, $CDCl_3$)

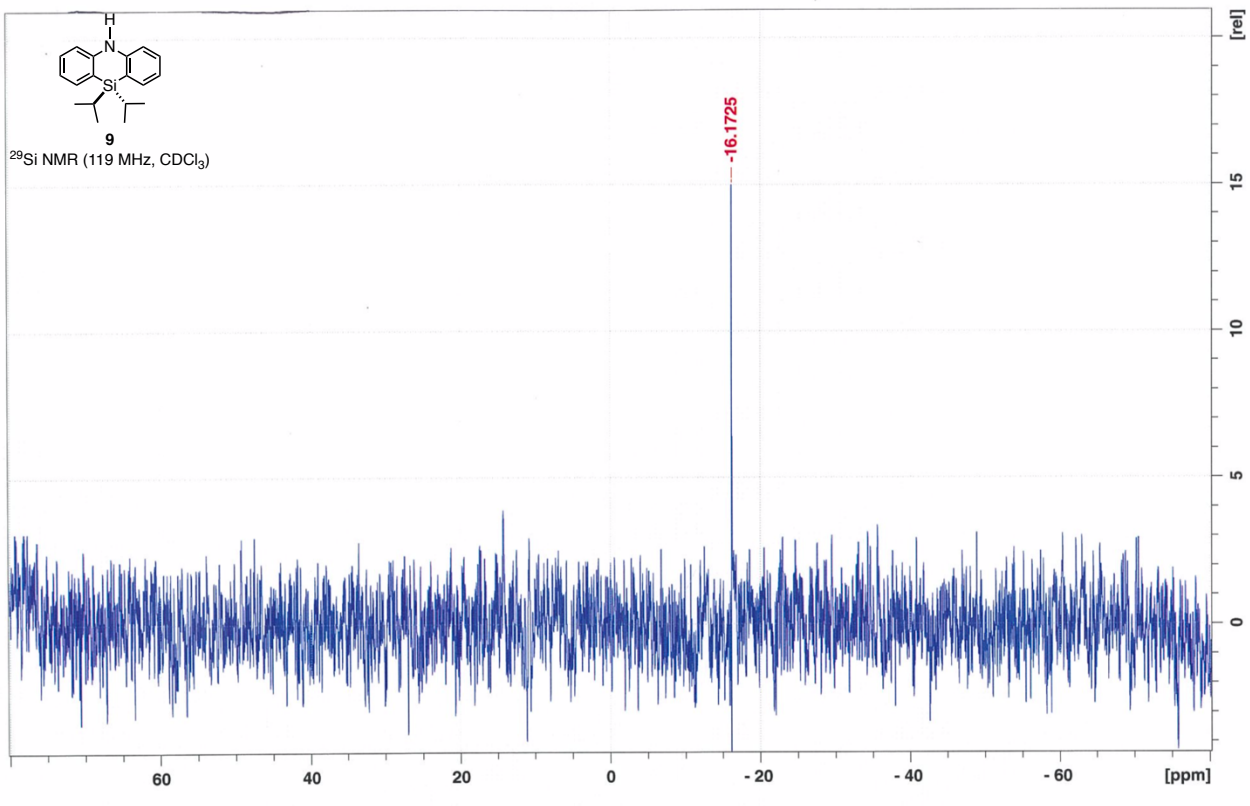
H
N
Si
9
^{29}Si NMR (119 MHz, $CDCl_3$)
-16.1725
[rel]
15
10
5
0
60
40
20
0
- 20
- 40
- 60
[ppm]

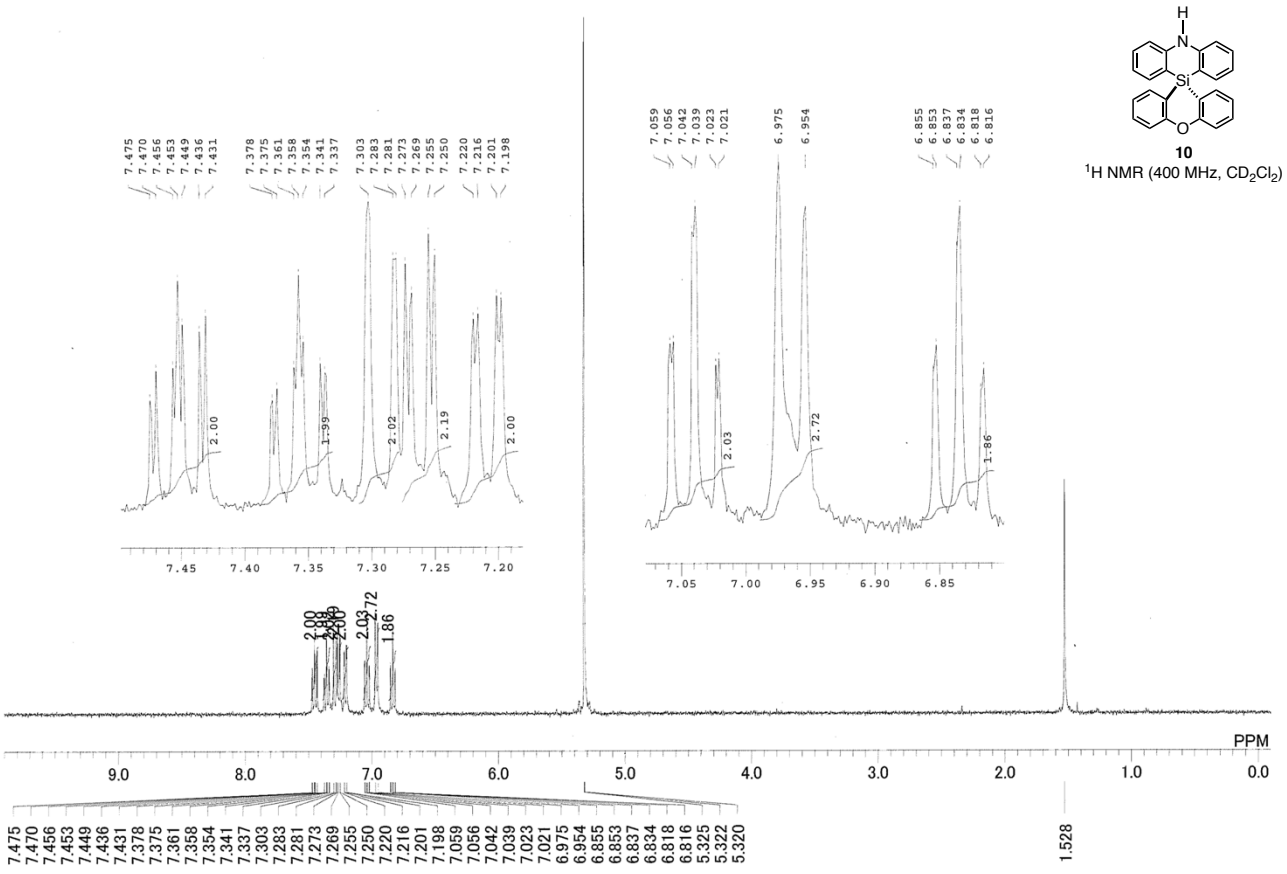
10
1H NMR (400 MHz, CD2Cl2)
PPM
1.528

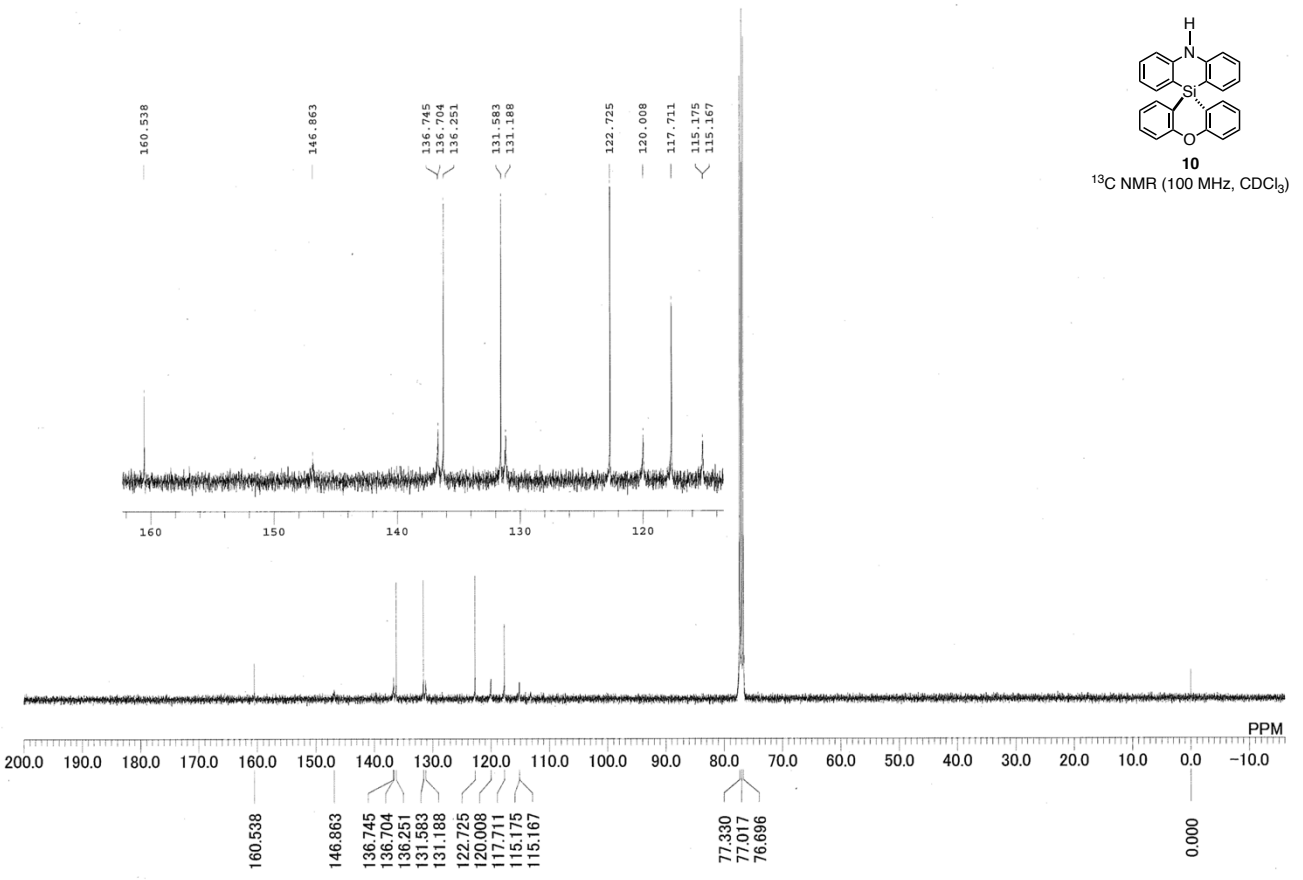
10
13C NMR (100 MHz, CDCl3)
PPM
160.538
146.863
136.745
136.704
136.251
131.583
131.188
122.725
120.008
117.711
115.175
115.167
77.330
77.017
76.696
0.000

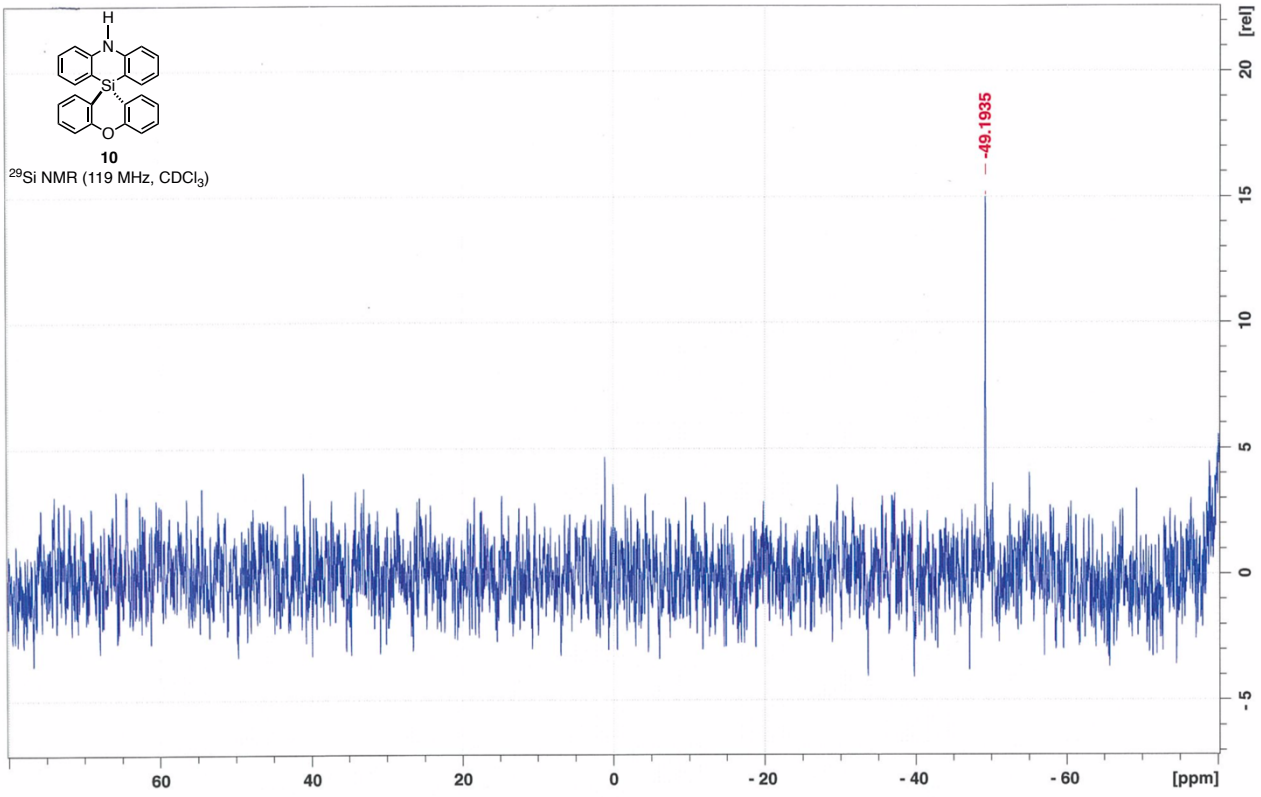
H
N
Si
O
10
29Si NMR (119 MHz, CDCl3)
-49.1935
[rel]
20
15
10
5
0
-5
60
40
20
0
- 20
- 40
- 60
[ppm]

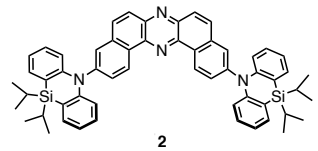

2

^{1}H NMR (400 MHz, $CDCl_3$)

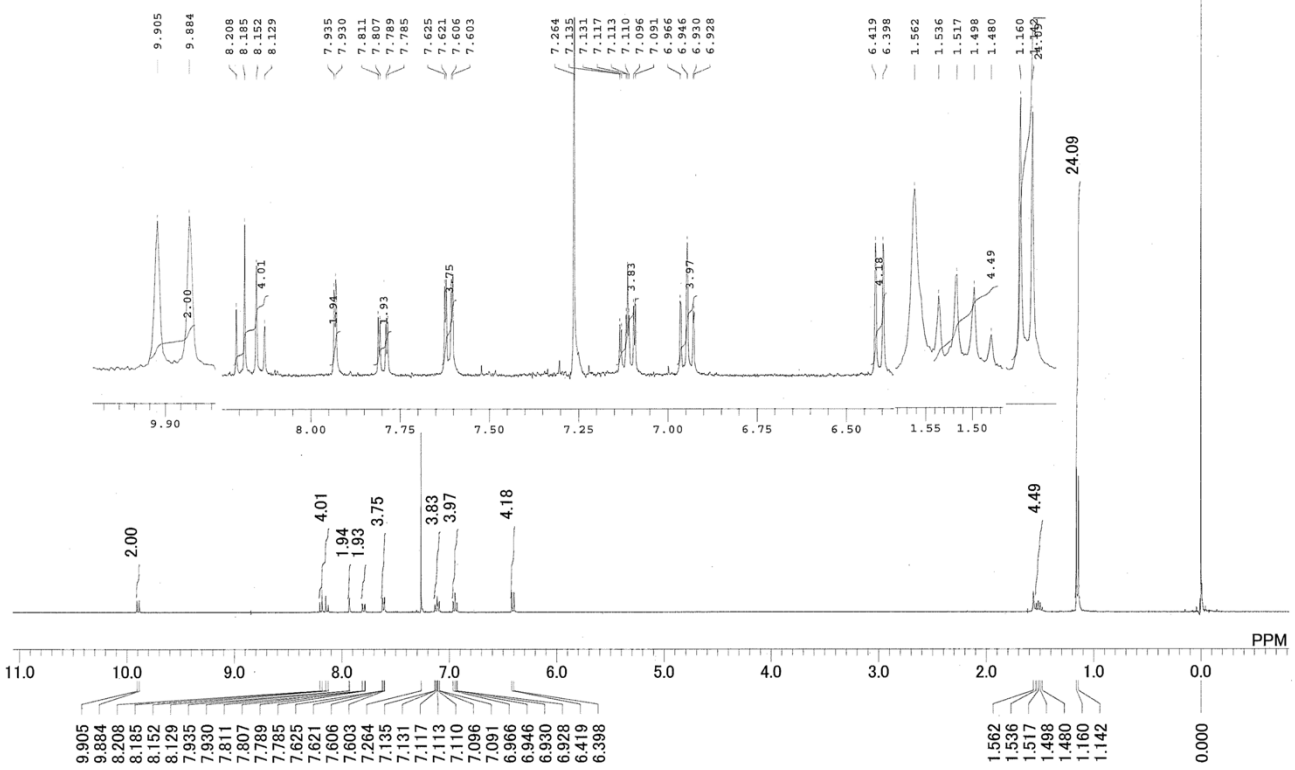

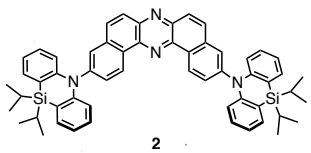

2

^{13}C NMR (100 MHz, $CDCl_3$)

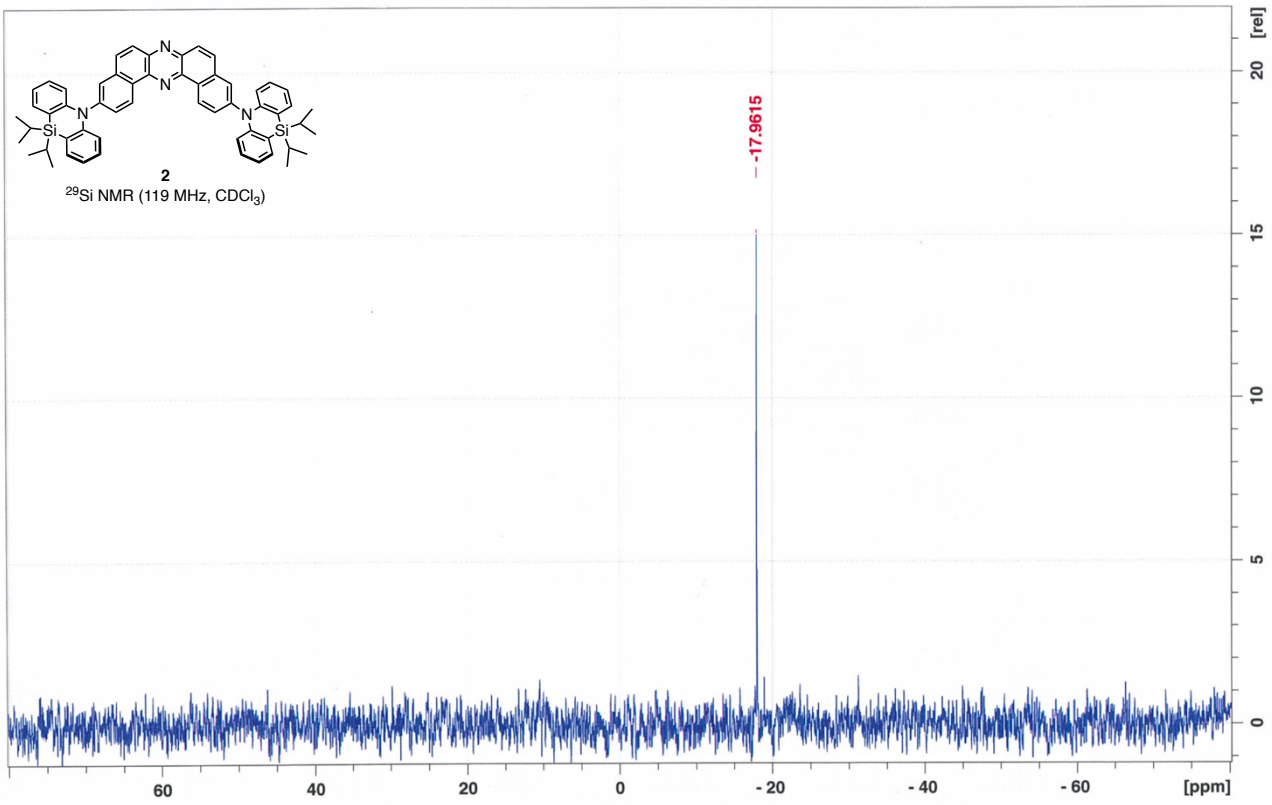
2
29Si NMR (119 MHz, CDCl3)
-17.9615
[rel]
20
15
10
5
0
60
40
20
0
- 20
- 40
- 60
[ppm]

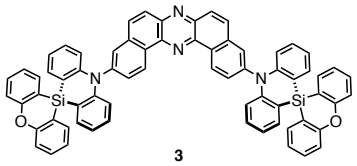

3

^{1}H NMR (400 MHz, $CDCl_3$)

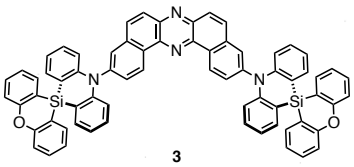

3

^{13}C NMR (100 MHz, $CDCl_3$)

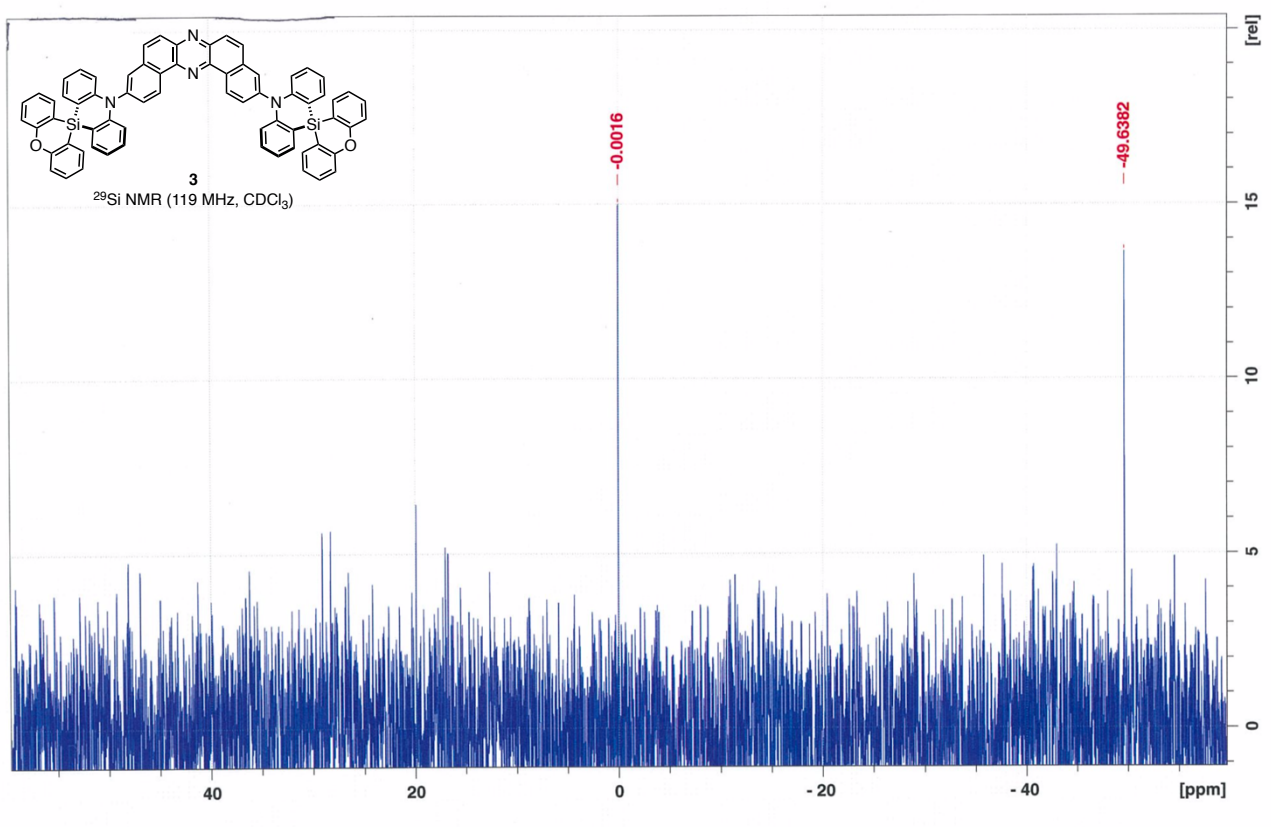
3
29Si NMR (119 MHz, CDCl3)
-0.0016
-49.6382
[rel]
15
10
5
0
40
20
0
- 20
- 40
[ppm]

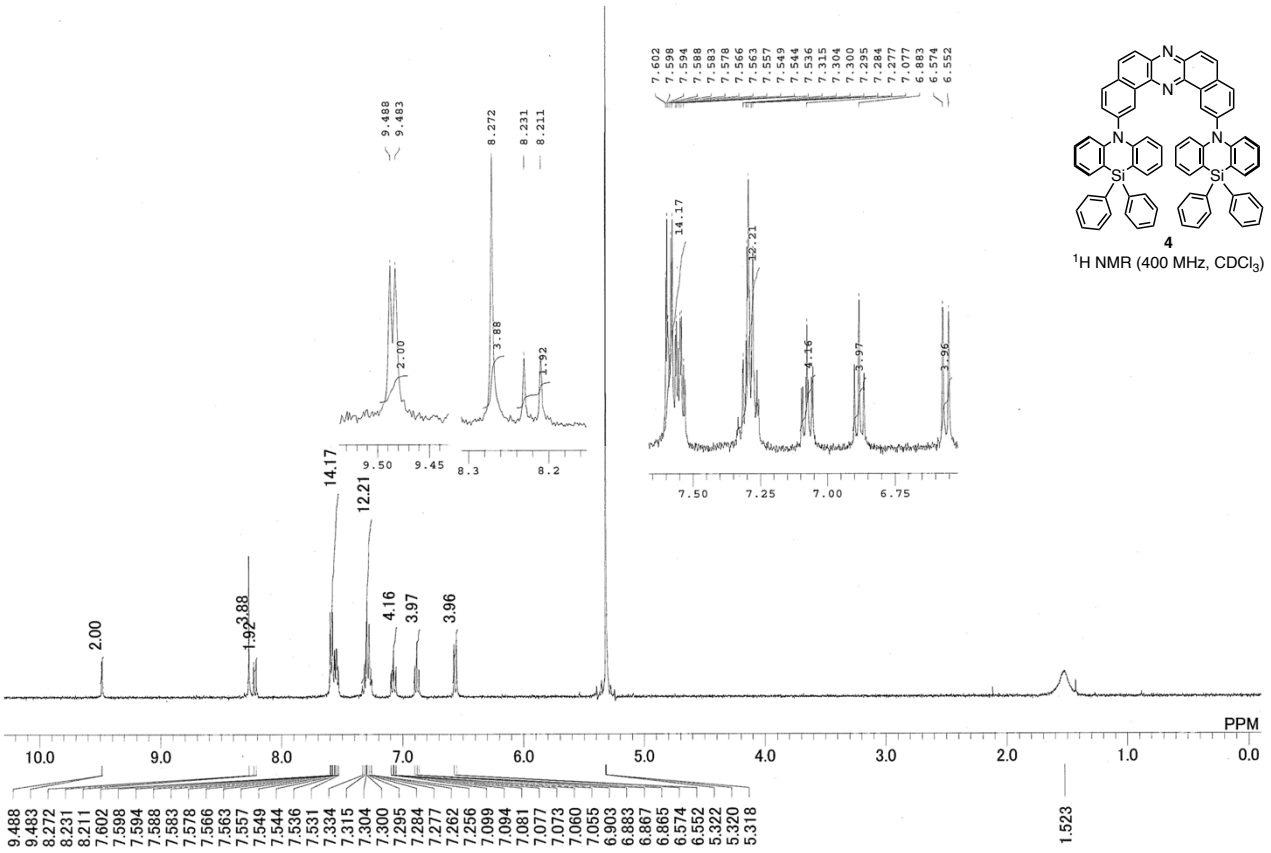
4
^{1}H NMR (400 MHz, $CDCl_3$)
PPM

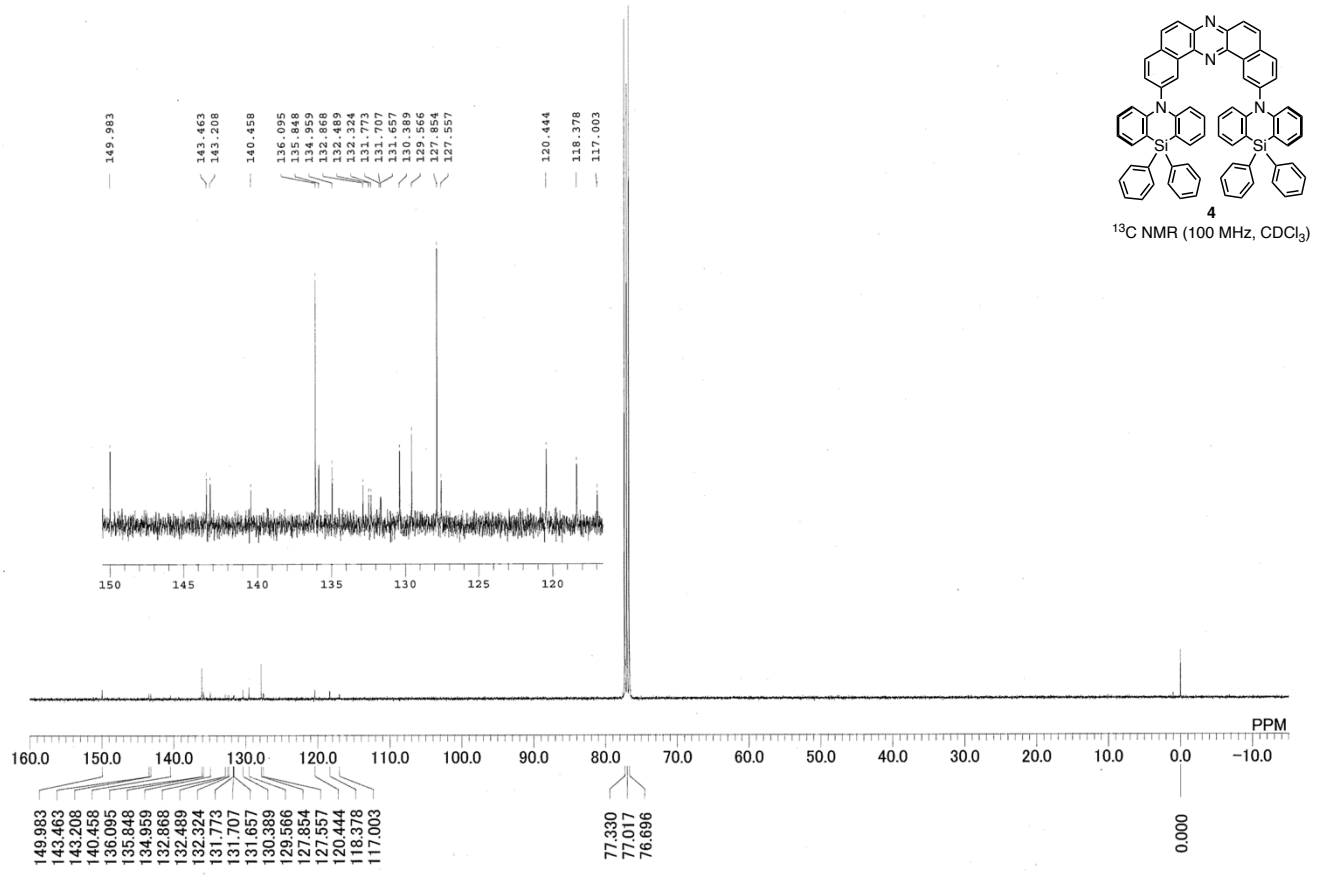
4
^{13}C NMR (100 MHz, $CDCl_3$)
PPM

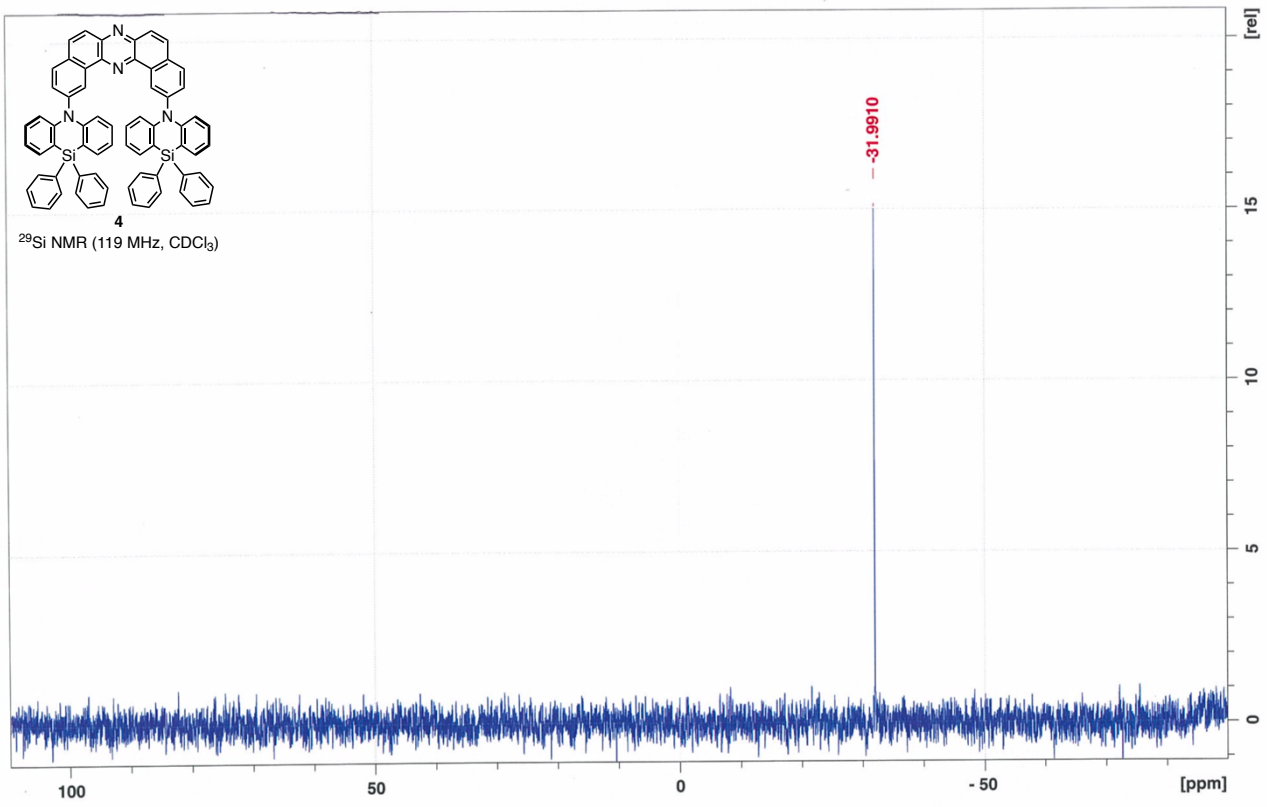
4
^{29}Si NMR (119 MHz, $CDCl_3$)
-31.9910
[rel]
15
10
5
0
100
50
0
- 50
[ppm]

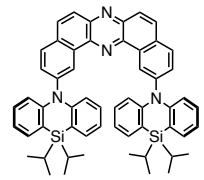

5

^{1}H NMR (400 MHz, $CDCl_3$)

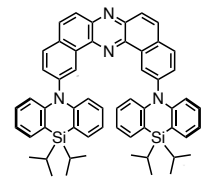

5

^{13}C NMR (100 MHz, $CDCl_3$)

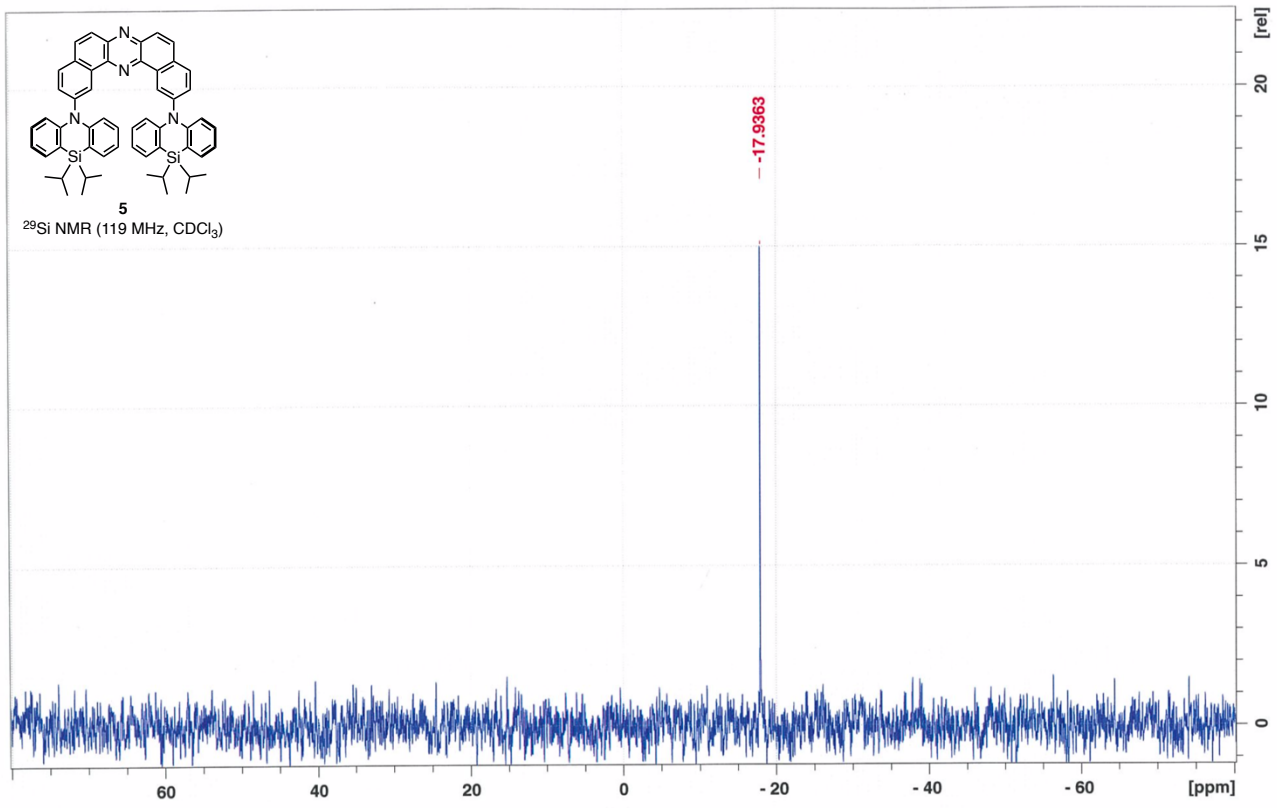

5

^{29}Si NMR (119 MHz, $CDCl_3$)

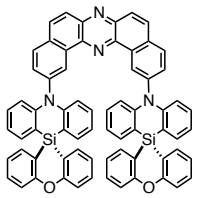

6

^{1}H NMR (400 MHz, $CDCl_3$)

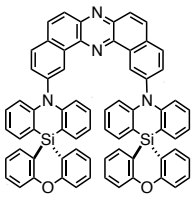

6

^{13}C NMR (100 MHz, $CDCl_3$)

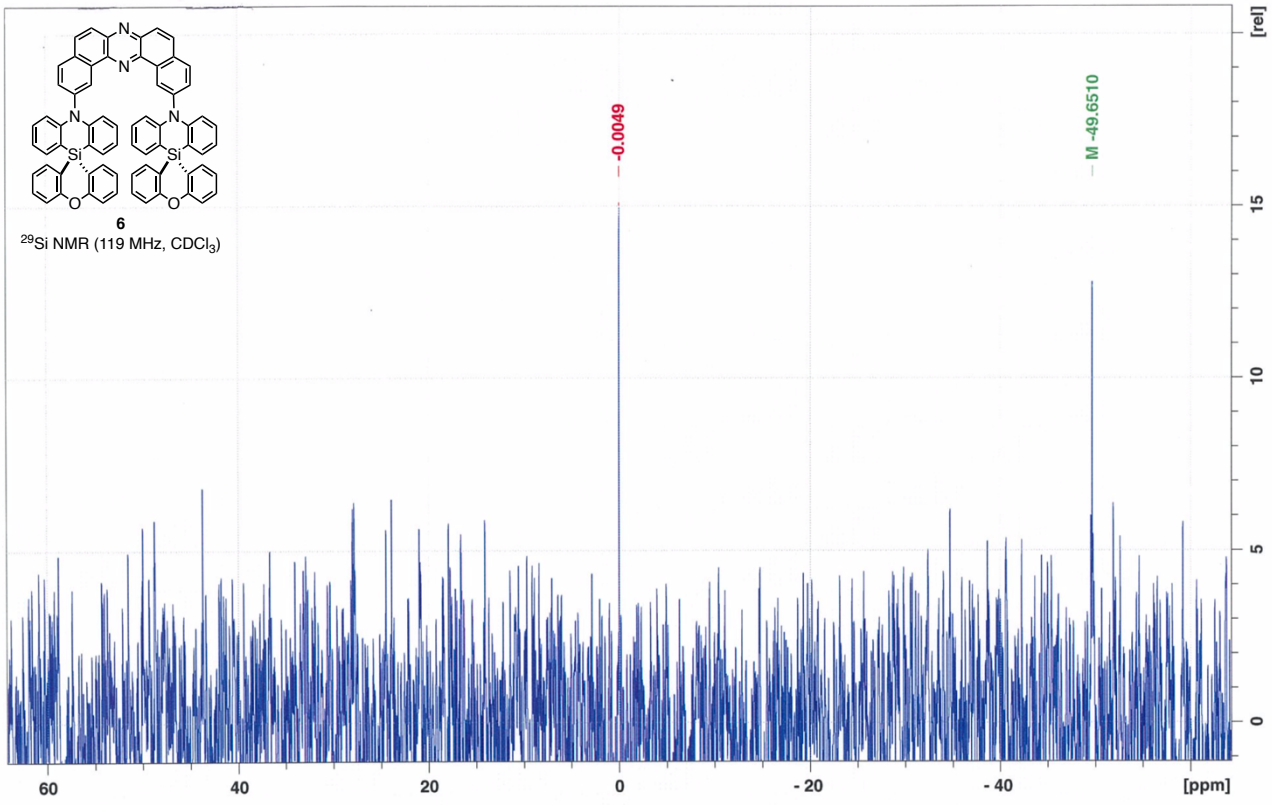
6
^{29}Si NMR (119 MHz, $CDCl_3$)
-0.0049
M -49.6510
[rel]
15
10
5
0
60
40
20
0
- 20
- 40
[ppm]

Theoretical Calculations

All DFT calculations were run with the LRC-ωPBE functional along with the 6-31G(d,p) basis set. The long-range separation parameter of the functional was tuned for each of the molecules following the procedure outlined in reference.[S10] The tuned parameters are shown in Table S1.

For excited state calculations, the Tamm-Dancoff (TDA) approximation was used,[S11] as it minimizes issues of triplet instability[S12] and is appropriate for spectrum simulations.[S13]

All DFT and TDA-DFT calculations were run with the QChem 5.2 package.[S14] Solvent effects were taken into account by means of the polarizable continuum model (PCM)[S15] using parameters for toluene.

Fluorescence, phosphorescence and ISC rates were estimated with the nuclear ensemble method, as implemented in the NEMO software interfaced with QChem 5.2. A total of 100 geometries were sampled taking as starting point the optimized geometries at S_1 and T_1 states for fluorescence and phosphorescence calculations, respectively. For rate estimations for the T_2 state, we made use of the geometries sampled for the T_1 state.

Functional Tuning

Table S3. Tuned values of the long range separation parameter for the different compounds.

Compound	ω (bohr^{-1})
1	0.169
2	0.169
3	0.169
4	0.166
5	0.169
6	0.163

Conformation Analysis

Probabilities were calculated using Boltzmann factors at 300 K as weights for each conformation.

Table S4 Probabilities (%) at 300 K associated with the different ground state, S_1 and T_1 conformations of compound **1**.

Conformation	S_0	S_1	T_1
eq-eq	91.4	97.4	0.5
eq-ax	8.3	2.6	99.0
ax-ax	0.2	0.0	0.5

Table S5 Probabilities (%) at 300 K associated with the different ground state, S_1 and T_1 conformations of compound **2**.

Conformation	S_0	S_1	T_1
eq-eq	99.6	99.5	0.6
eq-ax	0.4	0.5	99.4
ax-ax	0.0	0.0	0.0

Table S6 Probabilities (%) at 300 K associated with the different ground state, S_1 and T_1 conformations of compound **3**.

Conformation	S_0	S_1	T_1
eq-eq	97.4	99.1	2.5
eq-ax	2.5	0.9	97.2
ax-ax	0.0	0.0	0.3

Table S7 Probabilities (%) at 300 K associated with the different ground state, S_1 and T_1 conformations of compound **4**.

Conformation	S_0	S_1	T_1
eq-eq	74.5	0.0	0.0
eq-ax	25.5	100.0	100.0
ax-ax	0.0	0.0	0.0

Table S8 Probabilities (%) at 300 K associated with the different ground state, S_1 and T_1 conformations of compound **5**.

Conformation	S_0	S_1	T_1
eq-eq	85.4	0.1	0.0
eq-ax	14.6	99.9	100.0
ax-ax	0.0	0.0	0.0

Table S9 Probabilities (%) at 300 K associated with the different ground state, S_1 and T_1 conformations of compound **6**.

Conformation	S_0	S_1	T_1
eq-eq	92.1	0.2	0.0
eq-ax	7.9	99.8	100.0
ax-ax	0.0	0.0	0.0

Fluorescence Simulations

Table S10 Calculated fluorescence peaks (nm) for the 2,12-isomers in the eq-eq and eq-ax conformations.

Compound	eq-eq	eq-ax
4	481	528
5	493	512
6	487	547

Table S11 Calculated fluorescence peaks and rates in toluene for the 6 compounds in their preferred conformation in the S_1 state.

Compound	Fluorescence peak (nm)	Rate (s^{-1})
1	504	1E+07
2	524	1E+07
3	438	9E+06
4	528	8E+07
5	512	9E+07
6	547	9E+07

Phosphorescence Simulations

Table S12 Calculated T_1 phosphorescence peaks and rates in toluene for the 6 compounds in their preferred conformation in the T_1 state.

Compound	Phosphorescence peak (nm)	Rate (s^{-1})
1	686	5E+00
2	620	6E+00
3	573	5E+00
4	1426	1E+01
5	561	2E+01
6	754	7E+00

Table S13 Calculated T_2 phosphorescence peaks and rates in toluene for the 6 compounds in their preferred conformation in the T_1 state.

Compound	Phosphorescence peak (nm)	Rate (s^{-1})
1	493	2E+04
2	495	2E+03
3	456	3E+03
4	523	2E+03
5	525	5E+05
6	516	2E+04

Intersystem Crossing Rates

Table S14 Estimated ISC rates from the S_1 state for the 6 compounds in their preferred conformation in the S_1 state.

ISC	**1**	**2**	**3**	**4**	**5**	**6**
$S_1 \rightarrow T_1$	4E+07	5E-10	2E-06	1E+02	4E+02	9E+01
$S_1 \rightarrow T_2$	3E+10	3E+10	1E+10	1E+07	2E+09	2E+09
$S_1 \rightarrow T_3$	1E+09	5E+09	1E+10	5E+08	1E+09	1E+09
$S_1 \rightarrow T_4$	2E+04	2E+08	1E+10	5E+07	1E+08	2E+08
$S_1 \rightarrow T_5$	3E+05	3E+08	5E+09	8E+04	4E+05	4E+08

Table S15 Estimated rISC rates from the T_1 state for the 6 compounds in their preferred conformation in the T_1 state.

rISC	**1**	**2**	**3**	**4**	**5**	**6**
$T_1 \rightarrow S_1$	1E-05	2E-11	6E-02	6E-10	5E-07	1E-02
$T_1 \rightarrow S_2$	3E-09	2E-24	1E-05	5E-18	5E-16	1E-22
$T_1 \rightarrow S_3$	2E-20	1E-41	5E-17	2E-50	3E-35	3E-35
$T_1 \rightarrow S_4$	5E-25	2E-49	2E-21	8E-62	2E-61	2E-57
$T_1 \rightarrow S_5$	1E-37	3E-65	3E-29	1E-74	4E-77	1E-74

Table S16 Estimated rISC rates from the T_2 state for the 6 compounds in their preferred conformation in the T_1 state.

rISC	**1**	**2**	**3**	**4**	**5**	**6**
$T_2 \rightarrow S_1$	3E+08	1E+08	3E+07	2E+08	2E+10	1E+09
$T_2 \rightarrow S_2$	4E+01	1E-03	5E+01	2E+00	5E-04	5E-03
$T_2 \rightarrow S_3$	5E-03	1E-07	5E-03	2E-08	8E-28	6E-09
$T_2 \rightarrow S_4$	6E-04	4E-18	1E-05	3E-11	1E-29	2E-19

$T_2 \rightarrow S_5$	1E-11	1E-23	4E-10	3E-30	4E-94	5E-25

Average triplet gaps

Table S17 Average T_1-T_2 energy gaps (eV) for the 6 compounds in their preferred conformation in the T_1 state.

Gap	**1**	**2**	**3**	**4**	**5**	**6**
$T_1 \rightarrow T_2$	0.527	0.491	0.498	0.502	0.598	0.559

References

S1 M. Okazaki, Y. Takeda, P. Data, P. Pander, H. Higginbotham, A. P. Monkman and S. Minakata, *Chem. Sci.*, 2017, **8**, 2677–2686.

S2 Y.-K. Lim, J.-W. Jung, H. Lee and C.-G. Cho, *J. Org. Chem.*, 2004, **69**, 5778–5781.

S3 J. W. Sun, J. Y. Baek, K.-H. Kim, C.-K. Moon, J.-H. Lee, S.-K. Kwon, Y.-H. Kim and J.-J. Kim, *Chem. Mater.*, 2015, **27**, 6675–6681.

S4 M. Mamada, G. Tian, H. Nakanotani, J. Su and C. Adachi, *Angew. Chem. Int. Ed.*, 2018, **57**, 12380–12384.

S5 Rigaku Oxford Diffraction (2015), Software CrysAlisPro 1.171.39.5a Rigaku Corporation, Tokyo, Japan.

S6 SHELXT Version 2014/5. G. M. Sheldrick, *Acta Cryst.*, 2014, **A70**, C1437.

S7 CrystalStructure 4.3: Crystal Structure Analysis Package, Rigaku Corporation (2000-2018). Tokyo 196-8666, Japan.

S8 SHELXL Version 2018/1: G. M. Sheldrick, *Acta Cryst*., 2008, **A64**, 112–122.

S9 Olex2 (1.2): compiled 2018.05.29 svn.r3508 for OlexSys, GUI svn.r5506, *J. Appl*. *Cryst*. (2009). **42**, 339-341.

S10 T. Stein, L. Kronik and R. Baer, *J. Am. Chem. Soc.*, 2009, **131**, 2818–2820.

S11 S. Hirata and M. Head-Gordon, *Chem. Phys. Lett.*, 1999, **314**, 291–299.

S12 M. J. G. Peach, M. J. Williamson and D. J. Tozer, *J. Chem. Theory Comput.*, 2011, **7**, 3578–3585.

S13 A. Chantzis, A. D. Laurent, C. Adamo and D. Jacquemin, *J. Chem. Theory Comput.*, 2013, **9**, 4517–4525.

S14 Y. Shao and et al., *Mol. Phys.*, 2015, **113**, 184–215.

S15 G. Scalmani and M. J. Frisch, *J. Chem. Phys.*, 2010, **132**, 114110/1–15.